Genetic features of multicentric/multifocal intramucosal gastric carcinoma.

Aya Mizuguchi, Atsushi Takai, Takahiro Shimizu, Tomonori Matsumoto, Ken Kumagai, Shin'ichi Miyamoto, Hiroshi Seno, and Hiroyuki Marusawa

Department of Gastroenterology and Hepatology,

Graduate School of Medicine, Kyoto University, Kyoto, Japan

Short Title: Genetic features of multiple early gastric cancer.

Corresponding & Reprint Author: Hiroyuki Marusawa at:

Department of Gastroenterology and Hepatology,

Graduate School of Medicine, Kyoto University,

54 Kawara-cho, Shogoin, Sakyo-ku, Kyoto 606-8507, Japan

Phone; +81-75-751-4319, Fax; +81-75-751-4303

E-mail; maru@kuhp.kyoto-u.ac.jp

Key words: copy number aberration, early gastric cancer, heterogeneity, microsatellite instability, multiregional analysis

Abbreviations: CNAs: copy number aberrations, FFPE: formalin-fixed paraffin-embedded, *H. pylori*: *Helicobacter pylori*, MMR: mismatch repair, MSI: microsatellite instability, MSS: microsatellite stability

Article category: Cancer Genetics and Epigenetics, Research Article

Brief description: We determined the microsatellite instability and copy number aberrations in synchronous or metachronous multiple intramucosal early gastric cancers. Metachronous multiple intramucosal gastric carcinoma exhibit inter-tumor heterogeneity by individually acquiring genetic aberrations, while synchronous multiple gastric carcinomas could share partially common genetic alterations. Of note, gastric intramucosal carcinomas exhibit intra-tumor heterogeneity, including genetic alterations associated with avoidance of immune response at the very early stage of gastric carcinogenesis.

Funding: This work was supported by Japan Society for the Promotion of Science (JSPS) Grants-in-Aid for Scientific Research, KAKENHI [grant number 17H04158, 16K09357].

Disclosures: The authors have no conflicts of interest.

Abstract

Chronic gastritis caused by *Helicobacter pylori* (*H. pylori)* infection could lead to the development of gastric cancer. The finding that multiple gastric cancers can develop synchronously and/or metachronously suggests the development of field cancerization in chronically inflamed, *H. pylori*-infected gastric mucosa. The genetic basis of multiple tumorigenesis in the inflamed stomach, however, is not well understood. In this study, we analyzed the microsatellite instability (MSI) status and copy number aberrations (CNAs) of 41 multiple intramucosal early gastric cancers that synchronously or metachronously developed in 19 patients with *H. pylori* infection. Among the 41 intramucosal gastric carcinomas, 9 (22%) exhibited MSI, and the remaining 32 (78%) exhibited the microsatellite stable (MSS) phenotype. Metachronous multiple intramucosal gastric carcinoma exhibit inter-tumor heterogeneity by individually acquiring genetic aberrations. All synchronous multiple intramucosal gastric carcinoma pairs shared a common MSI/MSS profile, and CNA analysis revealed that synchronous multiple intramucosal gastric carcinoma pairs with the MSS phenotype shared common aberrations of representative tumor-suppressor genes, including focal deletion of *APC*, *TP53*, *CDKN2A*, and *CDKN2B*. Multiregional CNA analysis revealed that heterogeneous gene amplifications/deletions, including *PDL1* amplification, evolved under the presence of shared “trunk” genetic alterations in a subpopulation of individual intramucosal gastric carcinomas. These data suggest that multiple gastric carcinomas develop in a multicentric/multifocal manner exhibiting features of inter- and intra-tumor heterogeneity in *H. pylori*-infected gastric mucosa, whereas synchronous multiple intramucosal gastric carcinomas could share partially common genetic alterations, possibly via common oncogenic pathways.

Introduction

Chronic inflammation predisposes patients to the development of inflammation-associated cancer[1, 2]. Notably, tumors frequently develop in a multicentric manner in the background of chronically inflamed tissues. For example, hepatocellular carcinoma[3, 4] and colitis-associated colorectal cancers[5, 6] develop in a multicentric manner from tissues with chronic hepatitis and inflammatory bowel disease, respectively. These facts indicate that tissues exposed to chronic inflammation can acquire field cancerization as a basis of multi-centric tumorigenesis.

Gastric cancer is the fifth most common cancer and the third leading cause of cancer-related death worldwide[7]. The strongest risk factor for gastric cancer is *Helicobacter pylori* (*H. pylori*) infection and the resultant gastric inflammation[8, 9]. Interestingly, gastric cancers can frequently develop at multiple sites in patients with *H. pylori* infection. Indeed, we previously examined 255 *H. pylori*-infected cases with gastric epithelial neoplasia, including adenoma and intra-mucosal adenocarcinoma, and demonstrated that 19 cases (7.5%) developed synchronous multiple tumors and 43 cases (16.9%) developed a second gastric cancer metachronously[10]. Similarly, 8.7% and 5.2% of patients with early gastric cancer who underwent endoscopic resection developed synchronous and metachronous gastric cancers, respectively[11]. While these data suggest that chronically inflamed gastric mucosa with *H. pylori* infection provides the basis for multicentric/multifocal tumorigenesis, the molecular pathway of multiple tumor development in inflamed gastric mucosa remains unclear.

Cancer cells are generated through a stepwise accumulation of genetic aberrations, including somatic mutations, chromosomal rearrangements, and copy number aberrations (CNAs)[12,13]. Various factors, including reactive oxygen species and the activity of endogenous DNA mutator enzymes, mediate genetic aberrations during the process of

inflammation-associated tumorigenesis[14]. We previously demonstrated that aberrant expression of activation-induced cytidine deaminase (AID) is induced in response to *H. pylori* infection and the resultant pro-inflammatory cytokine stimulation in gastric epithelial cells, leading to the accumulation of somatic mutations in various tumor-related genes[15, 16]. Of note, aberrant AID activity induces not only somatic mutations, but also CNAs at various chromosomal loci in human gastric cells[17]. Our findings suggested that *H. pylori* infection could contribute to the occurrence of both somatic mutations and CNAs at the early stage of gastric tumorigenesis. On the other hand, The Cancer Genome Atlas (TCGA) project classified gastric cancers into four subtypes based on a comprehensive molecular evaluation; tumors positive for Epstein-Barr virus, tumors with microsatellite instability (MSI), tumors with chromosomal instability (CIN), and genomically stable tumors[18]. CIN-type tumors have extensive somatic CNAs and account for 50% of gastric cancer, whereas MSI type tumors exhibit hypermethylation and elevated mutation rates, and account for 22% of gastric cancer[18]. A previous study revealed that various CNAs are detectable in noninvasive gastric neoplasia, including gastric carcinoma *in situ* and adenoma[19]. It is unclear, however, whether genetic alterations, including MSI or CIN, are established at the early stage of *H. pylori*-related gastric tumorigenesis.

In the present study, to gain insight into the genetic pathways of multi-centric gastric carcinogenesis during the early stage, we determined the genetic features, including MSI status and CNAs, in tumor cells microscopically extracted from intramucosal gastric carcinomas that developed synchronously or metachronously in patients with *H. pylori* infection. In addition, to evaluate the intra-tumor heterogeneity at the early stage of gastric cancer development, we performed CNA analysis on multiple regions of a single intramucosal gastric carcinoma.

Materials and Methods

Study population, treatment methods, and follow-up strategy

We examined 25 patients with multiple intramucosal gastric carcinoma diagnosed at Kyoto University Hospital between 2007 and 2014. After excluding 6 cases due to insufficient tissue specimens, 41 samples from 19 patients were subjected to gene analyses. All the tumors were completely resected by endoscopic resection according to the criteria proposed by Gotoda et al[20]. The resected specimens were fixed with 10% formalin, embedded in paraffin, and examined histopathologically. All tumors were defined as lesions with prominent cellular atypia and severe architectural abnormalities within the mucosa, and no evidence of invasion into the submucosa was observed. According to the Vienna classification, the tumors were classified as intramucosal carcinoma (category 5.1)[21]. All tumors were reviewed by an experienced pathologist. Tumor location was categorized into the upper (U), middle (M), and lower (L) one-third parts of the stomach according to the Japanese Classification of Gastric Carcinoma guidelines[22]. All tumors were classified as the intestinal-type according to Lauren's classification[23]. Follow-up of the patients was performed by endoscopic examination of the upper gastrointestinal tract every 6-12 months after the initial resection.

We assessed the clinicopathologic variables, including patient age and sex, *H. pylori* infection confirmed by histologic examination or serum *H. pylori* IgG antibody, synchronous multiplicity of the primary neoplasia, histopathologic diagnosis at the initial endoscopic treatment, and development of metachronous multiple lesions. We defined synchronous multiplicity as lesions in regions separated by more than 10 mm of normal mucosa, which were defined before the initial resection or within 12 months after the initial resection. Because small synchronous lesions might be missed initially, metachronous multiple tumors were defined when the subsequent neoplasia was detected at a different site more than 12

months after the initial resection of the primary tumor(s).

The ethics committee of Kyoto University graduate school, Faculty of Medicine approved the study protocol, and all patients provided written informed consent for the use of specimens.

MSI analysis

To obtain tumor-specific DNA, formalin-fixed paraffin-embedded (FFPE) tissues were sliced consecutively at a 5-μm thickness. The tumor cell location was determined by hematoxylin and eosin staining of serial sections (Figure 1). Tumor and non-tumor samples were precisely extracted from the serial sections under microscopic visualization. Genomic DNA was extracted from these samples using a GeneRead DNA FFPE Kit (Qiagen, Valencia, CA). On average, 0.5 μg of DNA was obtained from each sample and subjected to genetic analyses. MSI analysis of the tumors and paired control of non-tumor tissues was performed using the MSI Analysis System Version 1.2 (Promega, Madison, WI) according to the manufacturer's protocol. Briefly, five mononucleotide repeat microsatellite markers (BAT-25, BAT-26, NR-21, NR-24, and MONO-27) were amplified with fluorescence-labeled primers and detection of the amplified fragments was performed on a 3130*xl* Genetic Analyzer (Applied Biosystems, Foster City, CA). The data were analyzed with GeneMapper Software Version 4.0 (Applied Biosystems). Allelic patterns for tumor and control pairs were compared and scored as MSI-positive if two or more novel alleles not found in the control were present in the tumor samples.

Immunohistochemistry

For histologic analysis, FFPE tissues were sectioned at a 5-μm thickness.

Immunohistochemistry was performed using anti-MLH1 (Ventana Medical Systems, Tucson, AZ), anti-PMS2 (Ventana Medical Systems), anti-MSH2 (Ventana Medical Systems), and anti-MSH6 (Abcam, Cambridge, MA) on a VENTANA DISCOVERY ULTRA research instrument (Ventana Medical Systems) according to the manufacturer's instructions. Visual assessment of the degree and intensity of the immunoreactivity was classified as no (-), weak (+), or strong positive staining (++) (Supplemental Figure 1).

Copy number aberration analyses

CNA analyses were performed using OncoScan CNV FFPE Assay Kit (Affymetrix, Santa Clara, CA) comprising approximately 240 thousand probes for each copy number. The size of each probe was approximately 40 bases and each probe was designed to include the single nucleotide polymorphism position. Molecular Inversion Probe (MIP) probes were hybridized to genomic DNA and split into two tubes containing paired nucleotide mixes (triphosphates of adenine + thymine or cytosine + guanine). In the presence of DNA polymerase and ligase, MIP probes circularize with their complementary nucleotide. Allele discrimination is enzymatically derived and highly specific, allowing for multiplexed assays[24]. The DNA (80 ng) was digested, amplified, purified, fragmented, labeled, and hybridized using an Affymetrix OncoScan Array GeneChip according to the manufacturer's instructions. Total and allele-specific copy numbers were determined using Nexus Express Software for OncoScan (Affymetrix). The percentage of CNAs in each chromosome arm was obtained by dividing the total length of CNAs of each chromosome arm by the whole length of the same chromosome arm.

Results

Characteristics of synchronous and metachronous multiple intramucosal gastric carcinomas that developed in patients with *H. pylori* infection.

We analyzed a total of 41 multiple intramucosal gastric carcinomas that developed synchronously or metachronously in 19 patients who received curative endoscopic resection of the tumors (Figure 1, Table 1, Supplemental Figure 2, Supplemental Tables 1&2). Patients included 14 men and 5 women aged 50-90 years (mean, 73.4), and all tumors developed in the background of atrophic gastritis mucosa due to *H. pylori* infection. Mean tumor size was 11.6 mm (range, 3-28), and all tumors were histologically diagnosed as well-differentiated (n=36) or moderately-differentiated (n=5) tubular adenocarcinoma. All tumors were within the mucosa and no invasion into the submucosa was observed. Among the 19 cases, 6 had synchronous multiple intramucosal gastric carcinoma and 13 had metachronous multiple intramucosal gastric carcinoma. Among the six synchronous cases, only one pair of tumors was found in the same geographical region of the stomach, although the distance between the tumors was more than 20 mm (Supplemental Table 1). Secondary tumors in metachronous cases were detected and endoscopically resected on average 38.3 months (range, 14-73) after the initial treatment (Supplemental Table 2). Among the 13 cases with metachronous intramucosal gastric carcinoma, *H. pylori* eradication was achieved in 6 after treatment of the primary tumor, although they developed secondary tumors (mean, 27.6 months; range, 9-47 months) after *H. pylori* eradication.

Synchronous multiple intramucosal gastric carcinomas in individual cases shared the common feature of either the MSS or MSI profile

To examine whether intramucosal early gastric cancer had already acquired either the MSS or MSI phenotype, we analyzed the MSS/MSI status in 41 intramucosal gastric carcinomas. MSI analysis revealed that 9 of 41 tumors (22%) exhibited the MSI phenotype,

while the remaining 32 tumors (78%) exhibited the MSS phenotype. Pairs of tumors that developed in two synchronous cases exhibited the MSI phenotype and the remaining four synchronous cases developed tumors with the MSS phenotype (Figure 2A, left panel), indicating that all six pairs of synchronous multiple intramucosal gastric carcinomas shared a common feature of either the MSS or MSI profile. On the other hand, MSI analysis also revealed that the allelic patterns for the paired tumors that developed in a synchronous manner were substantially different (data not shown), indicating that these paired tumors developed in a multicentric/multifocal manner, and not from the same origin. In contrast, 3 of 13 cases with metachronous multiple intramucosal gastric carcinoma exhibited a different MSI status between tumors, and only 1 case had the MSI phenotype in both tumors (Figure 2B, right panel). These findings suggested that synchronous multiple intramucosal gastric carcinoma in individual cases frequently shared the common feature of either the MSS or MSI profile.

To investigate whether the MSI phenotype observed in intramucosal gastric carcinoma was due to dysregulation of the mismatch repair (MMR) system, expression of four representative MMR proteins (MLH1, PMS2, MSH2, and MSH6) was examined by immunohistochemistry. First, we confirmed that all four MMR proteins were physiologically expressed in non-tumorous gastric epithelial cells in all cases examined (Supplemental Figure 3). The expression levels of MLH1 and PMS2 were concurrently decreased in 7 of 9 (78%) MSI-type intramucosal gastric carcinomas (Figure 2B, 2C). Only one pair of synchronous multiple intramucosal gastric carcinoma with the MSI phenotype (Case#1) expressed all four MMR proteins (Figure 2B, left panel). On the other hand, all MSS-type intramucosal gastric carcinomas expressed all four MMR proteins (Figure 2B, 2C), including two MSS-type tumors with increased expression of MMR proteins (Figure 2B, Supplemental Figure 4). These results suggested that the MSI phenotype occurred at the early stage of gastric cancer

development via the downregulation of MMR protein, and synchronous multiple intramucosal gastric carcinomas with the MSI phenotype could frequently develop via the dysregulated expression of common MMR proteins. Unfortunately, we could not evaluate the methylation status of the MLH1 promoter sequence because of the limited amount of DNA extracted from the FFPE tumor cells.

CNAs accumulated in intramucosal gastric carcinomas that developed in stomachs with *H. pylori* infection.

The TCGA project demonstrated that the majority of MSS gastric cancers, except Epstein-Barr virus-related gastric cancers, have the CIN phenotype[18]. To investigate CIN status at the early stage of gastric cancer development, we analyzed CNAs in intramucosal gastric carcinoma with the MSS or MSI phenotypes. We found that all intramucosal gastric carcinomas had a variety of CNAs throughout all the chromosomes (Figure 3, Supplemental Figure 5). Overall, copy number gain (14.3%) was more frequently observed than copy number loss (2.94%) in intramucosal gastric carcinoma with both the MSS and MSI phenotype, while copy number loss was relatively frequent in MSS tumors. For example, 7 of 32 (21.9%) MSS tumors had a comparatively high copy number loss of over 5% of the total chromosome length, whereas none of the MSI tumors showed the loss of these copy numbers (Figure 3, lower panel). Of note, the loss of 17p, including haplo-deficiency of *TP53*, was frequently found in 41% (13/32) of intramucosal gastric carcinomas with the MSS phenotype, but not in any intramucosal gastric carcinomas with the MSI phenotype (0/9; $p < 0.05$). In addition, a gain of 20p was observed in 69% (22/32) of intramucosal gastric carcinomas with the MSS phenotype compared with 22% (2/9) of intramucosal gastric carcinomas with the MSI phenotype ($p < 0.05$). On the other hand, in intramucosal gastric carcinoma with the MSI phenotype, a copy number gain was frequently observed (12.8%) compared with a copy

number loss (1.89%; $p < 0.001$; Figure 3). Particularly, the gain of 8p and 8q was detected in all MSI-type tumors, suggesting that the gain of 8p and 8q might be early oncogenic alterations during the development of MSI-type gastric cancer.

Taken together, various CNAs were present at the early stage of gastric cancer development. Intramucosal gastric carcinoma with the MSS phenotype exhibited a specific copy number loss, such as the 17p defect, whereas intramucosal gastric carcinoma with the MSI phenotype frequently exhibited the gain of 8p and 8q.

Inter-tumor heterogeneity and similarity of copy number aberrations in synchronous or metachronous multiple intramucosal gastric carcinomas.

To determine the similarities and/or differences in the genetic alterations that accumulated in multiply developed tumors, we compared CNAs in synchronous or metachronous multiple intramucosal gastric carcinomas. For this purpose, we focused on 30 representative cancer-related genes[18, 25, 26] and evaluated whether those genes were affected by CNAs in each tumor (Figure 4, Supplemental Figure 6). Among four cases of synchronous intramucosal gastric carcinoma with the MSS phenotypes, the paired tumors in three cases had common focal deletions of several representative tumor suppressor genes, including *APC* (5q22.2), *TP53* (17p13.1), *CDKN2A* (9p21.3), and *CDKN2B* (9p21.3), although the magnitude of the deleted chromosomal loci differed between tumors (Figure 4A, Supplemental Figure 6). On the other hand, 7 of 9 (77.8%) cases with metachronous tumors having the MSS phenotype exhibited no common focal aberrations of those representative tumor-related genes, except the common amplification of *MYC* (8q) or *GATA4* (8p) (Figure 4B, Supplemental Figure 6). Of note, none of the deletions of the representative tumor-suppressor genes was shared by 12 of the 13 (92.3%) metachronous cases, and 1 case (case#7) showed loss of the *APC* gene (Figure 4B).

These results suggested that gastric cancers could develop metachronously in the inflamed stomach with *H. pylori* infection in a multicentric/multifocal manner via various molecular pathways, whereas synchronous gastric cancers partially share common oncogenic pathways.

Intra-tumor heterogeneity of genetic alterations that evolved in intramucosal gastric carcinomas.

To study tumor evolution at the early stage of gastric carcinogenesis, four intramucosal gastric carcinomas with enough volume of tumor cells for further analysis were selected and copy number analysis of different geographic regions within a single tumor tissue was performed. Accordingly, multiregional tumor samples that were geographically separated from each other in a single tumor were dissected under microscopic visualization and subjected to comprehensive CNA analyses. Several CNAs were commonly shared by multiple tumor regions derived from the same intramucosal gastric carcinoma (Figure 5, Supplemental Figure 7). For example, 5q loss and 17p loss in Case#2 and 20q gain in Case #5 were commonly detected in all three regions of the same samples, and an 8q gain in Case#10 and Case#4 was commonly observed in both regions of the same samples. Of note, those commonly altered regions included representative tumor-related genes, including copy number losses of *APC* and *TP53* in the Case#2-1 tumors (Figure 5A) and *MYC* amplification in Cases #4 and #10 (Figure 5C, 5D). Similarly, a focal amplification of *GATA4* and *ZNF217* was a common feature in the samples of Cases #4 and #5, respectively (Figure 5B, 5D). On the other hand, tumor cells resided in a certain region that evolved individual CNAs in intramucosal gastric carcinoma tissues. Indeed, amplifications of several oncogenes, such as *epidermal growth factor receptor* (#2-1A) and *MET* (#5-1A), were detected in one region, but not in another part of a single tumor (#2-1B, #2-1C, #5-1B, and #5-1C; Figure 5A, 5B).

Interestingly, tumor cells derived from a subpopulation of intramucosal gastric carcinomas acquired *PDL1* amplification in two tumors (#2-1A and #5-1B; Figure 5A, 5B).

Together, multiregional copy number analysis revealed that intra-tumor heterogeneity was already developed in intramucosal early gastric cancer under the basis of common "trunk" CNAs. The findings that tumor cells with amplification of the *PDL1* locus were detectable in a subset of tumorous regions indicate that cancer cells associated with anti-tumor therapy evolved as a subpopulation of tumor cells at the early stage of gastric cancer development.

Discussion

Chronic gastritis associated with *H. pylori* infection is an established risk factor for carcinogenesis. To understand the genetic pathway of the development of multiple gastric cancers in the stomach with *H. pylori* infection, we analyzed the genetic landscape of synchronous and metachronous multiple early gastric cancers using intramucosal gastric carcinoma samples dissected microscopically from FFPE tissue specimens. Our results indicated that metachronous multiple intramucosal gastric carcinomas possessed a variety of CNAs as well as MSI features, suggesting the tumorigenesis in a multicentric/multifocal manner. In addition, synchronous multiple intramucosal gastric carcinomas frequently shared a common feature of the MSI/MSS profile as well as the copy number losses of the common tumor suppressor genes at the early stage of tumorigenesis.

Evaluation of the actual risk of multiple tumorigenesis in gastric cancer patients with *H. pylori* infection receiving a total or subtotal gastrectomy has been difficult because these patients have no or only post-operative remnant stomachs after surgery. Recent progress in endoscopic techniques has allowed for the treatment of gastric cancers by minimally invasive procedures that maintain the major portion of the gastric mucosa in the same condition as

before the treatment of primary neoplasia[27, 28]. In the present study, we demonstrated that 9 of 41 (22%) multiple intramucosal gastric carcinomas exhibited the MSI phenotype, while 32 (78%) had the MSS phenotype. The TCGA project of gastric cancer genome analyses demonstrated that 50% of advanced gastric cancers are classified as the CIN type corresponding to the putative MSS phenotype, while MSI type accounted for 22%[18]. Other studies also revealed that 14% to 34% of gastric cancers exhibit the MSI phenotype[29-31]. Together, our findings indicate that the MSI phenotype could be established in cancer cells at the early stage of tumorigenesis in patients with *H. pylori* infection. On the other hand, MSI is largely caused by hypermethylation of the *MLH1* gene promoter in sporadic gastric cancers[32]. Consistently, we found that 7 of 9 (78%) MSI-type intramucosal gastric carcinomas had decreased expression of MLH1 and PMS2 protein, indicating that most MSI-type gastric cancers that developed in stomachs infected with *H. pylori* acquired the MSI phenotype due to the downregulation of MLH1 expression at the early stage of tumorigenesis.

In contrast to MSI-type tumors, somatic CNAs are frequently observed in gastric cancers with the MSS phenotype[18, 33]. Comprehensive molecular analysis of advanced gastric cancers with various etiologies revealed that arm-level copy number gains are detectable on chromosomes 8q (60%) and 20q (65%), and losses are detectable on chromosomes 18p (45%), 4q (40%), and 21q (40%)[18]. Deng et al. showed that the frequency of amplified broad chromosomal regions was 9.8% to 33.7%, whereas deleted chromosomal regions were detected in 7.8% to 13.0% of advanced gastric cancers[25]. CNA analyses of gastric carcinoma *in situ* and dysplasia previously showed that the 8q gain was frequently detectable in high-grade adenoma[19]. We demonstrated here that arm-level copy number alterations at various chromosomal loci have already evolved during the early stage of intramucosal gastric carcinoma. Of note, we found that most MSS-type intramucosal gastric carcinomas exhibited

a relatively low frequency of CNAs compared with those observed in the previously reported CIN-type advanced gastric cancers[18]. These results suggest that a number of CNAs could accumulate as gastric cancer progresses from the early stage to the advanced stage, leading to the development of typical CIN-type tumors.

The results of the present study demonstrated that synchronously developed multiple intramucosal gastric carcinomas shared the common feature of the MSI/MSS phenotype. In addition, some of the representative tumor-related genes were commonly altered by copy number changes in the majority of synchronous multiple intramucosal gastric carcinomas. For example, 5q22, including the *APC* gene, and 9p21.3, including the *CDKN2A/2B* genes, were commonly deleted in both tumors that developed in Cases #6 and #14, respectively. The common deletion of 17p13.1, including the *TP53* gene, was found in multiple tumors that developed in two cases (Cases #8 and #16). In Case #16, the *RB1* gene located in 13q14.2 was also deleted in both tumors. On the other hand, the overall CNA landscape was substantially different in the paired synchronously developed tumors, indicating that those tumors did not derive from the same origin. These findings suggested that synchronously developed gastric cancers could partially share the same oncogenic pathway in patients with *H. pylori* infection, and those tumors could acquire additional genetic alterations caused by several etiologic factors during tumor evolution. In contrast, the finding that most metachronous multiple intramucosal gastric carcinomas frequently lacked the common genetic features assessed by MSI and CNA analysis suggested that *H. pylori*-associated gastric cancer could also emerge via different oncogenic pathways in a multi-centric manner.

It was recently revealed that intra-tumor heterogeneity plays an important role in the lethal outcome of cancer, therapeutic failure, and drug resistance[34-37]. The intra-tumor heterogeneity determined in colorectal cancers provides the putative process of clonal evolution[35]. Li et al. recently constructed an endogenous molecular network of gastric cancers

that contributes to intra-tumor heterogeneity[38]. Ongoing linear and branching evolution caused by genetic alterations results in multiple simultaneous subclones that may individually give rise to episodes of disease relapse and metastasis by environmental selection pressures[37]. In the present study, we examined intra-tumor heterogeneity appearing as CNAs in intramucosal gastric carcinomas using multiregional tumor sampling. Notably, alterations of the representative cancer-related genes, including loss of *APC* and *TP53* (Case #2) and gain of *MYC* (Cases #4 and #10), were commonly detectable in multiregional tumor samples, suggesting that these common alterations are putative founder changes occurring at the initial stage of tumorigenesis. On the other hand, several CNAs were not common among the regions in identical intramucosal tumors, suggesting the existence of intra-tumor copy number variations at the early stage of gastric carcinogenesis. Interestingly, CNAs associated with anti-tumor therapy emerged in a subset of tumor tissues. For example, *EGFR* amplification was detected in a subpopulation of tumors in Case #2. Of note, *PDL1* amplification was found in a subpopulation of tumor cells in Cases #2 and #5. Recently, antibody-mediated blockade of the PD-L1/PD-1 pathway received attention as a novel immunotarget therapy effective against various types of cancers[39]. Kim et al. demonstrated that PD-L1 expression was detected in more than 40% of patients with gastric cancers[40]. The KEYNOTE-012 study revealed that 22% of patients with PD-L1–positive recurrent or metastatic advanced gastric cancer achieve a partial response by the administration of the anti-PD-1 antibody pembrolizumab[41]. Kataoka et al. demonstrated that structure variations disrupting 3'-untranslated regions of the *PDL1* gene cause aberrant expression of PD-L1 in multiple cancers, including gastric cancer[42]. Our results imply that a subpopulation of gastric cancer cells acquired genetic alterations associated with avoidance of the immune response even at the early stage of tumorigenesis, possibly contributing to the evolution of immunotherapy-resistant tumor cells.

In summary, we demonstrated that multiple intramucosal gastric carcinomas exhibited substantial inter- and intra-tumor heterogeneity with the evolution of various genetic alterations, including the emergence of a subpopulation of tumor cells with the putative ability of immune escape. In addition, synchronous multiple intramucosal gastric carcinomas in the stomach with *H. pylori* infection frequently shared a common genetic profile, such as the MSI/MSS phenotypes and CNA of the representative tumor-related gene loci, suggesting a common molecular pathway for tumorigenesis in each individual. Further examination of the clonal evolution of the cancer genome is necessary to clarify the molecular basis of the high risk for multiple gastric cancer development in chronically inflamed stomach with underlying *H. pylori* infection. In addition, to clarify whether the profile of genetic alterations depends on the etiology of the gastric tumorigenesis, it would also be important to unveil the genetic features of gastric cancers developed in the stomach without *H. pylori* infection.

Acknowledgments

We thank S. Minamiguchi for histologic examination.

References

1. Grivennikov SI, Greten FR, Karin M. Immunity, inflammation, and cancer. *Cell* 2010;**140**: 883-99.

2. Chiba T, Marusawa H, Ushijima T. Inflammation-associated cancer development in digestive organs: mechanisms and roles for genetic and epigenetic modulation. *Gastroenterology* 2012;**143**: 550-63.

3. Marquardt JU, Andersen JB, Thorgeirsson SS. Functional and genetic deconstruction of the cellular origin in liver cancer. *Nat Rev Cancer* 2015;**15**: 653-67.

4. Takeda H, Takai A, Inuzuka T, Marusawa H. Genetic basis of hepatitis virus-associated

hepatocellular carcinoma: linkage between infection, inflammation, and tumorigenesis. *J Gastroenterol* 2017;**52**: 26-38.

5. Leedham SJ, Graham TA, Oukrif D, McDonald SA, Rodriguez-Justo M, Harrison RF, Shepherd NA, Novelli MR, Jankowski JA, Wright NA. Clonality, founder mutations, and field cancerization in human ulcerative colitis-associated neoplasia. *Gastroenterology* 2009;**136**: 542-50 e6.

6. Galandiuk S, Rodriguez-Justo M, Jeffery R, Nicholson AM, Cheng Y, Oukrif D, Elia G, Leedham SJ, McDonald SA, Wright NA, Graham TA. Field cancerization in the intestinal epithelium of patients with Crohn's ileocolitis. *Gastroenterology* 2012;**142**: 855-64 e8.

7. Ferlay J, Soerjomataram I, Dikshit R, Eser S, Mathers C, Rebelo M, Parkin DM, Forman D, Bray F. Cancer incidence and mortality worldwide: sources, methods and major patterns in GLOBOCAN 2012. *Int J Cancer* 2015;**136**: E359-86.

8. Uemura N, Okamoto S, Yamamoto S, Matsumura N, Yamaguchi S, Yamakido M, Taniyama K, Sasaki N, Schlemper RJ. Helicobacter pylori infection and the development of gastric cancer. *N Engl J Med* 2001;**345**: 784-9.

9. Polk DB, Peek RM, Jr. Helicobacter pylori: gastric cancer and beyond. *Nat Rev Cancer* 2010;**10**: 403-14.

10. Aoi T, Marusawa H, Sato T, Chiba T, Maruyama M. Risk of subsequent development of gastric cancer in patients with previous gastric epithelial neoplasia. *Gut* 2006;**55**: 588-9.

11. Kato M, Nishida T, Yamamoto K, Hayashi S, Kitamura S, Yabuta T, Yoshio T, Nakamura T, Komori M, Kawai N, Nishihara A, Nakanishi F, et al. Scheduled endoscopic surveillance controls secondary cancer after curative endoscopic resection for early gastric cancer: a multicentre retrospective cohort study by Osaka University ESD study group. *Gut* 2013;**62**: 1425-32.

12. Shimizu T, Marusawa H, Endo Y, Chiba T. Inflammation-mediated genomic instability:

roles of activation-induced cytidine deaminase in carcinogenesis. *Cancer Sci* 2012;**103**: 1201-6.

13. Vogelstein B, Kinzler KW. Cancer genes and the pathways they control. *Nat Med* 2004;**10**: 789-99.

14. Alexandrov LB, Nik-Zainal S, Wedge DC, Aparicio SA, Behjati S, Biankin AV, Bignell GR, Bolli N, Borg A, Borresen-Dale AL, Boyault S, Burkhardt B, et al. Signatures of mutational processes in human cancer. *Nature* 2013;**500**: 415-21.

15. Matsumoto Y, Marusawa H, Kinoshita K, Endo Y, Kou T, Morisawa T, Azuma T, Okazaki IM, Honjo T, Chiba T. Helicobacter pylori infection triggers aberrant expression of activation-induced cytidine deaminase in gastric epithelium. *Nat Med* 2007;**13**: 470-6.

16. Shimizu T, Marusawa H, Matsumoto Y, Inuzuka T, Ikeda A, Fujii Y, Minamiguchi S, Miyamoto S, Kou T, Sakai Y, Crabtree JE, Chiba T. Accumulation of somatic mutations in TP53 in gastric epithelium with Helicobacter pylori infection. *Gastroenterology* 2014;**147**: 407-17 e3.

17. Matsumoto Y, Marusawa H, Kinoshita K, Niwa Y, Sakai Y, Chiba T. Up-regulation of activation-induced cytidine deaminase causes genetic aberrations at the CDKN2b-CDKN2a in gastric cancer. *Gastroenterology* 2010;**139**: 1984-94.

18. Cancer Genome Atlas Research N. Comprehensive molecular characterization of gastric adenocarcinoma. *Nature* 2014;**513**: 202-9.

19. Uchida M, Tsukamoto Y, Uchida T, Ishikawa Y, Nagai T, Hijiya N, Nguyen LT, Nakada C, Kuroda A, Okimoto T, Kodama M, Murakami K, et al. Genomic profiling of gastric carcinoma in situ and adenomas by array-based comparative genomic hybridization. *J Pathol* 2010;**221**: 96-105.

20. Gotoda T, Yanagisawa A, Sasako M, Ono H, Nakanishi Y, Shimoda T, Kato Y. Incidence of lymph node metastasis from early gastric cancer: estimation with a large number of cases

at two large centers. *Gastric Cancer* 2000;**3**: 219-25.

21. Schlemper RJ, Riddell RH, Kato Y, Borchard F, Cooper HS, Dawsey SM, Dixon MF, Fenoglio-Preiser CM, Flejou JF, Geboes K, Hattori T, Hirota T, et al. The Vienna classification of gastrointestinal epithelial neoplasia. *Gut* 2000;**47**: 251-5.

22. Japanese classification of gastric carcinoma: 3rd English edition. *Gastric Cancer* 2011;**14**: 101-12.

23. Lauren P. The Two Histological Main Types of Gastric Carcinoma: Diffuse and So-Called Intestinal-Type Carcinoma. An Attempt at a Histo-Clinical Classification. *Acta Pathol Microbiol Scand* 1965;**64**: 31-49.

24. Thompson PA, Ljuslinder I, Tsavachidis S, Brewster A, Sahin A, Hedman H, Henriksson R, Bondy ML, Melin BS. Loss of LRIG1 locus increases risk of early and late relapse of stage I/II breast cancer. *Cancer Res* 2014;**74**: 2928-35.

25. Deng N, Goh LK, Wang H, Das K, Tao J, Tan IB, Zhang S, Lee M, Wu J, Lim KH, Lei Z, Goh G, et al. A comprehensive survey of genomic alterations in gastric cancer reveals systematic patterns of molecular exclusivity and co-occurrence among distinct therapeutic targets. *Gut* 2012;**61**: 673-84.

26. Liang L, Fang JY, Xu J. Gastric cancer and gene copy number variation: emerging cancer drivers for targeted therapy. *Oncogene* 2016;**35**: 1475-82.

27. Goto O, Fujishiro M, Kodashima S, Ono S, Omata M. Outcomes of endoscopic submucosal dissection for early gastric cancer with special reference to validation for curability criteria. *Endoscopy* 2009;**41**: 118-22.

28. Isomoto H, Shikuwa S, Yamaguchi N, Fukuda E, Ikeda K, Nishiyama H, Ohnita K, Mizuta Y, Shiozawa J, Kohno S. Endoscopic submucosal dissection for early gastric cancer: a large-scale feasibility study. *Gut* 2009;**58**: 331-6.

29. dos Santos NR, Seruca R, Constancia M, Seixas M, Sobrinho-Simoes M. Microsatellite

instability at multiple loci in gastric carcinoma: clinicopathologic implications and prognosis. *Gastroenterology* 1996;**110**: 38-44.

30. Yamamoto H, Perez-Piteira J, Yoshida T, Terada M, Itoh F, Imai K, Perucho M. Gastric cancers of the microsatellite mutator phenotype display characteristic genetic and clinical features. *Gastroenterology* 1999;**116**: 1348-57.

31. Falchetti M, Saieva C, Lupi R, Masala G, Rizzolo P, Zanna I, Ceccarelli K, Sera F, Mariani-Costantini R, Nesi G, Palli D, Ottini L. Gastric cancer with high-level microsatellite instability: target gene mutations, clinicopathologic features, and long-term survival. *Hum Pathol* 2008;**39**: 925-32.

32. Leung SY, Yuen ST, Chung LP, Chu KM, Chan AS, Ho JC. hMLH1 promoter methylation and lack of hMLH1 expression in sporadic gastric carcinomas with high-frequency microsatellite instability. *Cancer Res* 1999;**59**: 159-64.

33. Wang K, Yuen ST, Xu J, Lee SP, Yan HH, Shi ST, Siu HC, Deng S, Chu KM, Law S, Chan KH, Chan AS, et al. Whole-genome sequencing and comprehensive molecular profiling identify new driver mutations in gastric cancer. *Nat Genet* 2014;**46**: 573-82.

34. Andor N, Graham TA, Jansen M, Xia LC, Aktipis CA, Petritsch C, Ji HP, Maley CC. Pan-cancer analysis of the extent and consequences of intratumor heterogeneity. *Nat Med* 2016;**22**: 105-13.

35. Uchi R, Takahashi Y, Niida A, Shimamura T, Hirata H, Sugimachi K, Sawada G, Iwaya T, Kurashige J, Shinden Y, Iguchi T, Eguchi H, et al. Integrated Multiregional Analysis Proposing a New Model of Colorectal Cancer Evolution. *PLoS Genet* 2016;**12**: e1005778.

36. McGranahan N, Swanton C. Clonal Heterogeneity and Tumor Evolution: Past, Present, and the Future. *Cell* 2017;**168**: 613-28.

37. Yates LR, Campbell PJ. Evolution of the cancer genome. *Nat Rev Genet* 2012;**13**: 795-806.

38. Li S, Zhu X, Liu B, Wang G, Ao P. Endogenous molecular network reveals two mechanisms of heterogeneity within gastric cancer. *Oncotarget* 2015;**6**: 13607-27.

39. Brahmer JR, Tykodi SS, Chow LQ, Hwu WJ, Topalian SL, Hwu P, Drake CG, Camacho LH, Kauh J, Odunsi K, Pitot HC, Hamid O, et al. Safety and activity of anti-PD-L1 antibody in patients with advanced cancer. *N Engl J Med* 2012;**366**: 2455-65.

40. Kim JW, Nam KH, Ahn SH, Park DJ, Kim HH, Kim SH, Chang H, Lee JO, Kim YJ, Lee HS, Kim JH, Bang SM, et al. Prognostic implications of immunosuppressive protein expression in tumors as well as immune cell infiltration within the tumor microenvironment in gastric cancer. *Gastric Cancer* 2016;**19**: 42-52.

41. Muro K, Chung HC, Shankaran V, Geva R, Catenacci D, Gupta S, Eder JP, Golan T, Le DT, Burtness B, McRee AJ, Lin CC, et al. Pembrolizumab for patients with PD-L1-positive advanced gastric cancer (KEYNOTE-012): a multicentre, open-label, phase 1b trial. *Lancet Oncol* 2016;**17**: 717-26.

42. Kataoka K, Shiraishi Y, Takeda Y, Sakata S, Matsumoto M, Nagano S, Maeda T, Nagata Y, Kitanaka A, Mizuno S, Tanaka H, Chiba K, et al. Aberrant PD-L1 expression through 3'-UTR disruption in multiple cancers. *Nature* 2016;**534**: 402-6.

Figure Legends

Figure 1. The images of endoscopy and histology of multiple intramucosal gastric carcinomas.

Representative endoscopic images and histologic examination of multiple intramucosal gastric carcinomas. All tumors were resected endoscopically and evaluated histologically based on hematoxylin and eosin staining. Tumors are located in the surrounding regions as indicated by the blue dotted line in the endoscopic images. (A) Two intramucosal gastric carcinomas developed synchronously in Case #1. One (#1-2-1) was located in the middle part of the stomach (elevated type, 12x12 mm in diameter) and histology showed well-differentiated tubular adenocarcinoma. Another (#1-2-2) was located in the lower part (elevated type, 6x3 mm in diameter) and histology showed well-differentiated tubular adenocarcinoma. (B) Two intramucosal gastric carcinomas developed metachronously in Case #9. The first lesion (#9-1) developed in the middle part of the stomach (depressed type, 10x10 mm in diameter) and histology showed well-differentiated tubular adenocarcinoma. The second tumor (#9-2) developed in the lower part of the stomach (depressed type, 11x6 mm in diameter) and was resected 45 months after the initial resection of tumor #9-1. Histology showed well-differentiated tubular adenocarcinoma. Scale bars are 500 μm.

Figure 2. MSS/MSI status of synchronous or metachronous multiple intramucosal gastric carcinomas.

(A) Schematic images of MSS/MSI classification of synchronous (left panel) or metachronous (right panel) multiple intramucosal gastric carcinomas. (B) MMR protein expression in synchronous (left panel) or metachronous (right panel) multiple intramucosal gastric carcinomas by immunohistochemical analysis. The intensity of immunoreactivity was classified as no staining (-), weak (+), or strong positive staining (++). (C)

Immunohistochemistry of representative intramucosal gastric carcinoma samples for four MMR proteins, including MLH1, PMS2, MSH2, and MSH6. Scale bars are 100 μm.

Figure 3. Copy number aberration (CNA) of multiple intramucosal gastric carcinomas.

Heat map of copy number aberrations (CNAs) determined in 41 intramucosal gastric carcinomas of 19 cases. (A) Copy number gain. (B) Copy number loss. The proportion of the altered region on each chromosome arm is shown as a colored box with gradation.

Figure 4. Focal amplifications or deletions of the representative tumor-suppressor genes in synchronous or metachronous multiple intramucosal gastric carcinomas.

Focal amplifications or deletions of the representative tumor-suppressor genes in (A) synchronous and (B) metachronous multiple intramucosal gastric carcinomas. Green highlighted samples show the MSS phenotype and yellow highlighted samples show the MSI phenotype. Red and blue boxes represent corresponding gene amplification and deletion, respectively.

Figure 5. Focal amplifications or deletions of the representative tumor-related genes in multi-regions of each single intramucosal gastric carcinomas.

Focal gene amplification or deletion in multiregional tumor samples was determined by CNA analyses. Endoscopic images of intramucosal gastric carcinoma (left panels) and focal amplification or deletion of the representative tumor-related genes (right panels) in #2-1 (A), #5-1 (B), #10-2 (C), and #4-2(D) are shown. Tumors are located in the surrounding regions by the blue dotted line in the endoscopic images. The letters on the image correspond to the samples on the chart. Red and blue boxes represent corresponding gene amplification and deletion, respectively.

Figure 1.

A Case1

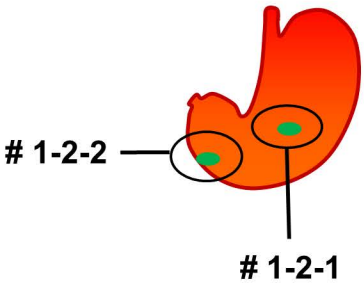

#1-2-1（12×12mm）

#1-2-2（6×3mm）

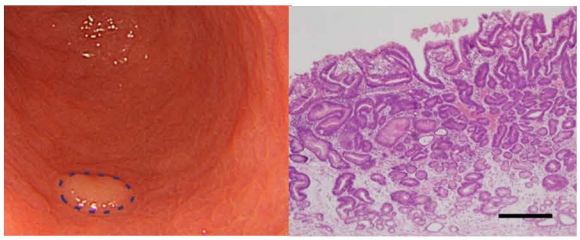

B Case9

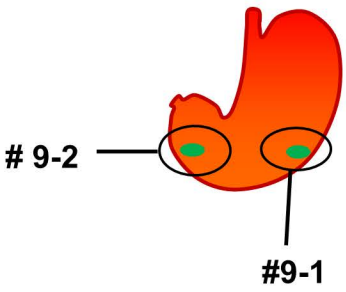

#9-1（10×10mm）

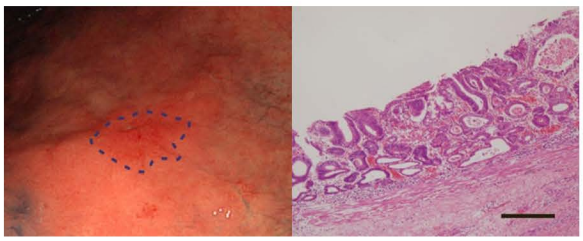

#9-2（ 11×6mm ）

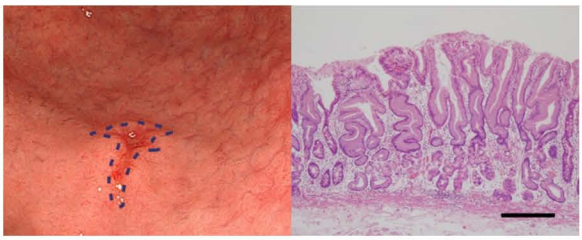

Figure 2.

A

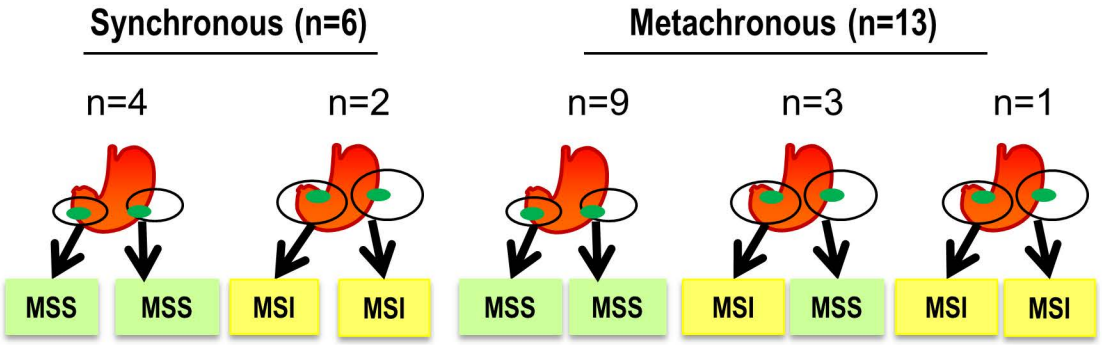

B

Synchronous

Case	MSI/ MSS	Immunohistochemistry			
		MLH1	PMS2	MSH2	MSH6
# 1-2-1	MSI	++	++	++	++
# 1-2-2	MSI	+	+	+	+
# 16-2-1	MSI	–	–	+	+
# 16-2-2	MSI	–	–	+	+
# 8-1-1	MSS	+	+	+	+
# 8-1-2	MSS	+	+	+	+
# 11-1-1	MSS	++	++	++	++
# 11-1-2	MSS	+	+	+	+

Metachronous

Case	MSI/ MSS	Immunohistochemistry			
		MLH1	PMS2	MSH2	MSH6
# 13-1	MSI	–	–	+	+
# 13-2	MSI	–	–	+	+
# 9-1	MSS	++	+	+	+
# 9-2	MSS	++	++	+	+
# 14-1	MSS	+	+	+	+
# 14-2	MSS	++	++	+	+
# 17-1	MSS	+	+	+	+
# 17-2	MSI	–	–	+	+
# 18-1	MSS	+	+	+	+
# 18-2	MSI	–	–	+	+
# 3-1	MSI	–	–	+	+
# 3-2	MSS	++	++	++	++

C

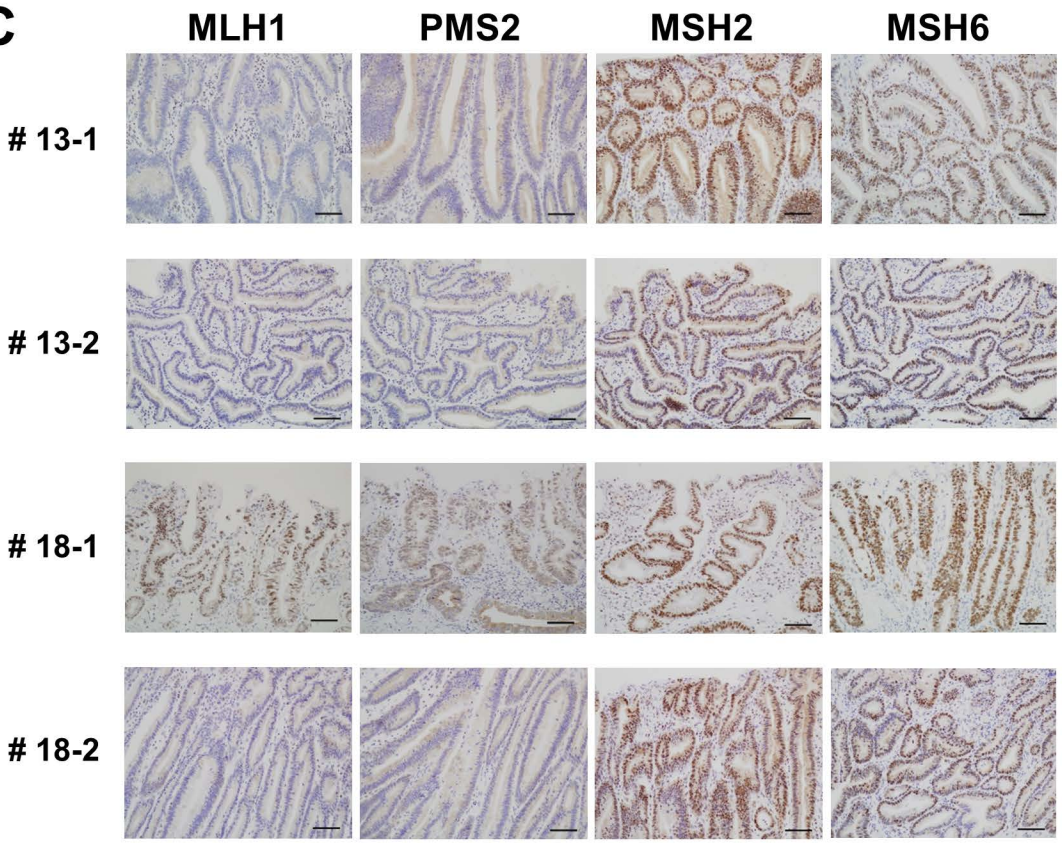

Figure 3.

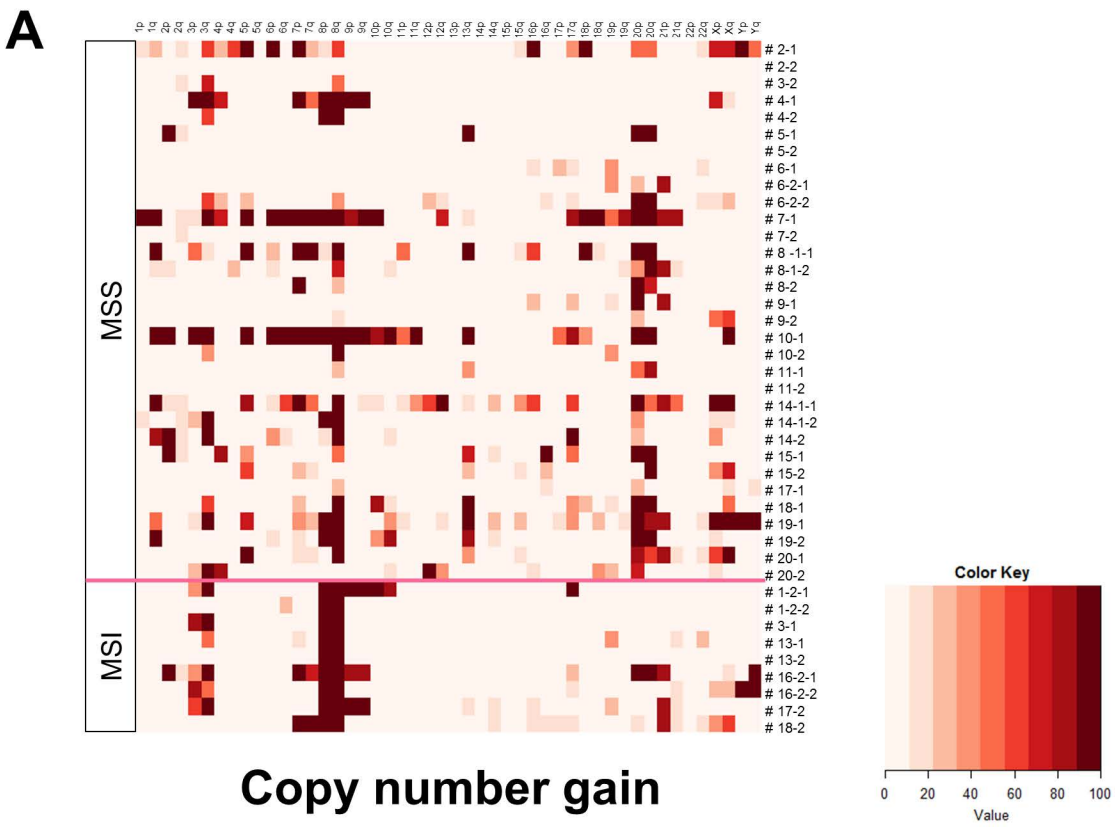
A
MSS
MSI
2-1
2-2
3-2
4-1
4-2
5-1
5-2
6-1
6-2-1
6-2-2
7-1
7-2
8 -1-1
8-1-2
8-2
9-1
9-2
10-1
10-2
11-1
11-2
14-1-1
14-1-2
14-2
15-1
15-2
17-1
18-1
19-1
19-2
20-1
20-2
1-2-1
1-2-2
3-1
13-1
13-2
16-2-1
16-2-2
17-2
18-2
Color Key
0
20
40
60
80
100
Value
Copy number gain

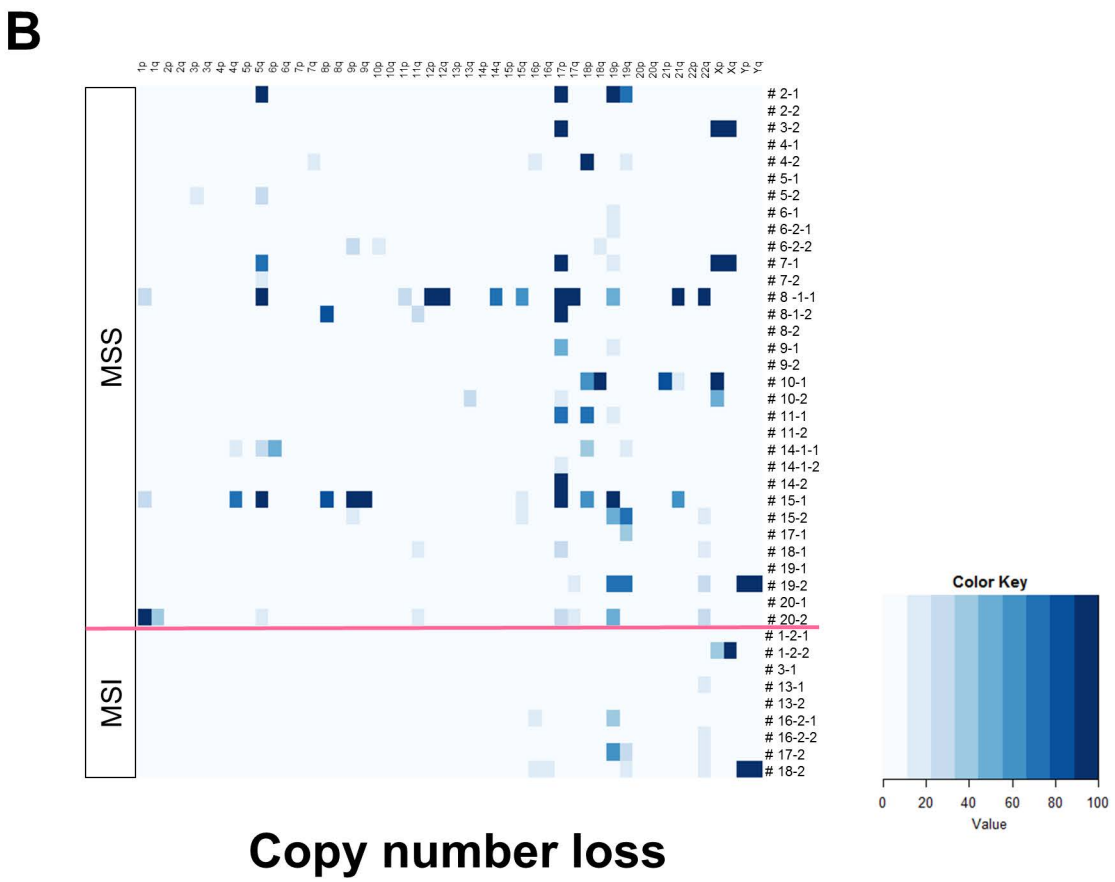
B
MSS
MSI
2-1
2-2
3-2
4-1
4-2
5-1
5-2
6-1
6-2-1
6-2-2
7-1
7-2
8 -1-1
8-1-2
8-2
9-1
9-2
10-1
10-2
11-1
11-2
14-1-1
14-1-2
14-2
15-1
15-2
17-1
18-1
19-1
19-2
20-1
20-2
1-2-1
1-2-2
3-1
13-1
13-2
16-2-1
16-2-2
17-2
18-2
Color Key
0
20
40
60
80
100
Value
Copy number loss

Figure 4.

A **Synchronous GCs**

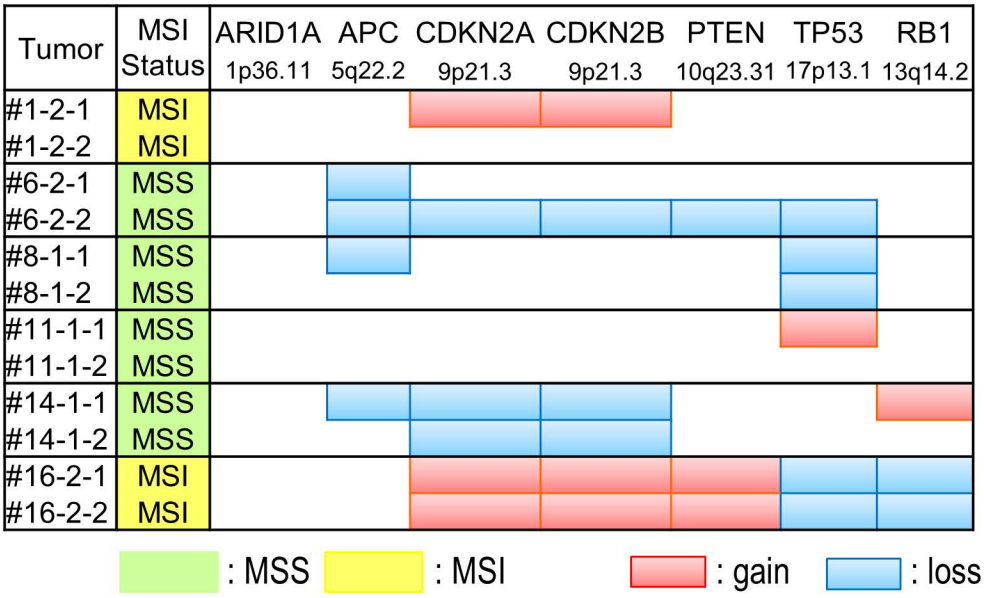

B **Metachronous GCs**

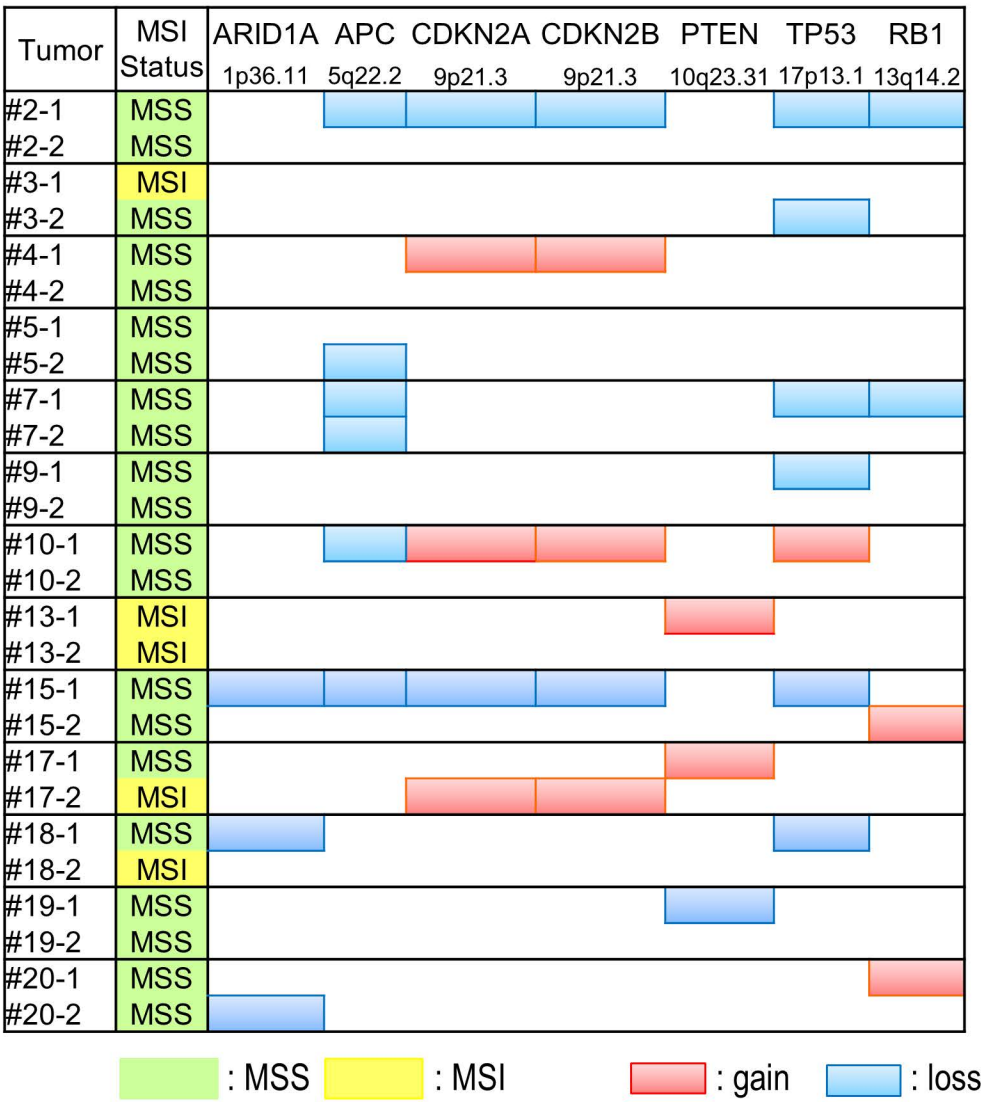

Figure 5.

A

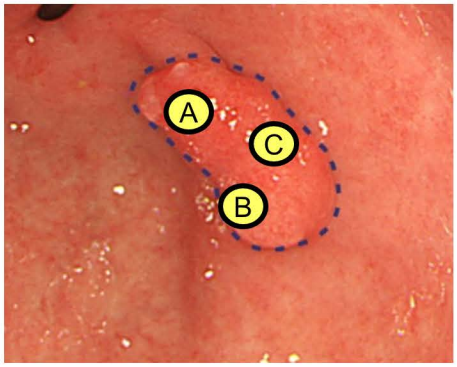

#2-1（18 × 16mm）

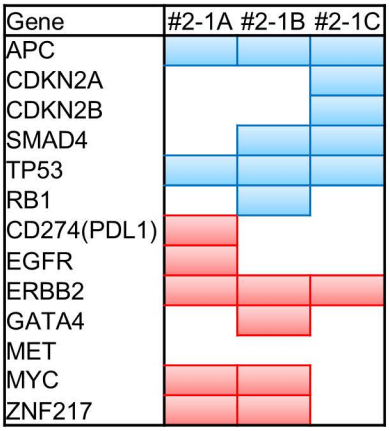

B

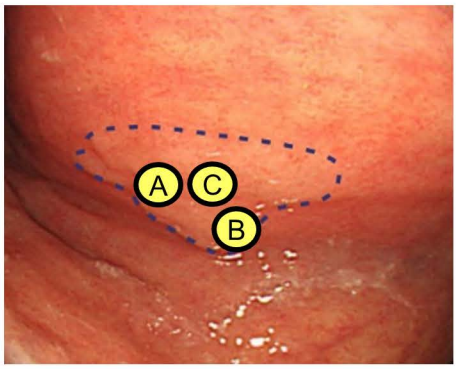

#5-1（14 × 11mm）

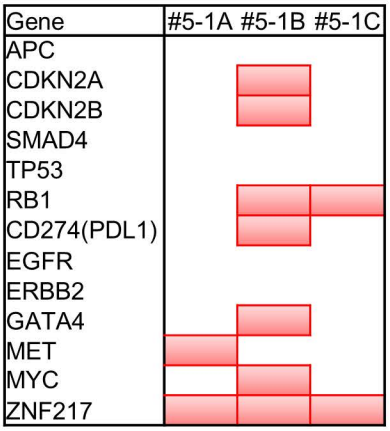

C

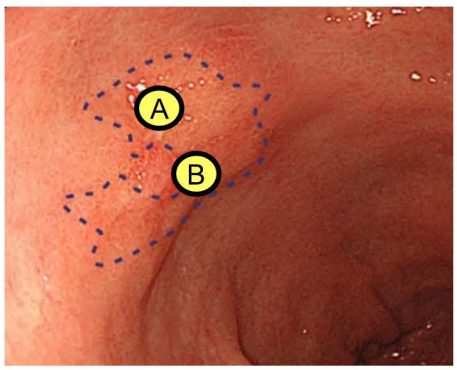

#10-2（28 × 26mm）

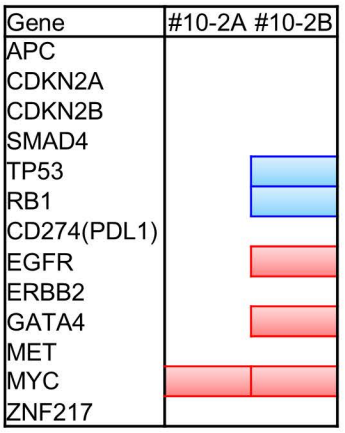

D

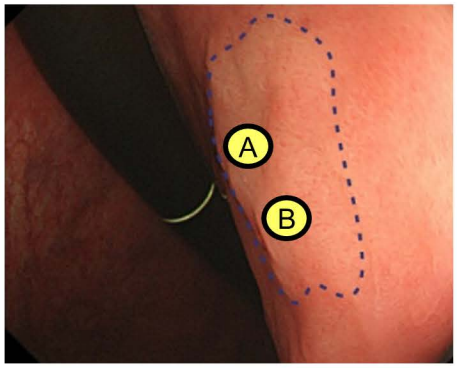

#4-2（18 × 16mm）

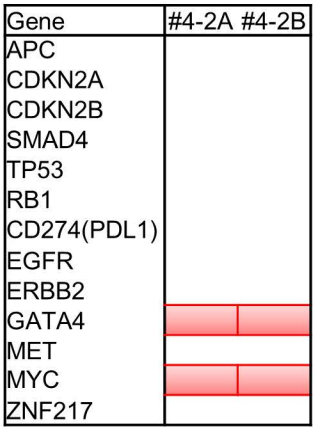

: gain

: loss

Table 1.

Clinicopathological information of patients with synchronous or metachronous multiple intramucosal gastric carcinomas

	Total	Synchronous	Metachronous
Number of patients, n	19	6	13
Male sex, n (%)	14 (73.7)	5 (83.3)	9 (69.2)
Age, mean (range)	73.4 (50-90)	74.1 (66-85)	73.1 (50-90)
Number of tumors, n	41	12	29
Locus, n (%)			
U	8 (20)	2(17)	6 (21)
M	11 (27)	4(33)	7 (24)
L	22 (54)	6(50)	16 (55)
Macroscopic type, n (%)			
Protruding	3 (7.3)	0 (0)	3 (10)
Elevated	15 (36.6)	6 (60)	9 (31)
Flat	1 (2.4)	0 (0)	1 (3.4)
Depressed	22 (53.7)	6 (40)	16 (55)
Histological type, n (%)			
Well differenciated	36 (87.8)	10 (83)	26 (90)
Moderately differenciated	5 (20)	2 (17)	3 (10)
Papillary	0 (0)	0 (0)	0 (0)
Tumor size (major axis), mm, mean (range)	11.6 (3-28)	11.8 (3-22)	11.5 (5-28)

Supplemental Figure 1. The immunoreactivity classification of histologic analyses.

Visual assessment of the degree and intensity of the immunoreactivity against MLH1, PMS2, MSH2 and MSH6 was classified as no (-), weak (+), or strong positive staining (++). The representative images for each immunoreactivity classification were shown. There were no tumor samples without any expression of MSH2 and MSH6. Scale bars are 100 μm.

Supplemental Figure 2. The images of endoscopy and histology of multiple intramucosal gastric carcinomas.

Endoscopic and histologic images of all gastric carcinomas used in this study, except Case #1 and #9 are shown. Tumors are located in the surrounding regions as indicated by the blue dotted line in the endoscopic images and the sizes of tumors are described. Tumors were evaluated histologically based on hematoxylin and eosin staining. Scale bars in the histologic images are 500 μm.

Supplemental Figure 3. Immunohistochemistry for four MMR proteins in non-tumorous gastric mucosa.

Expression of MLH1, PMS2, MSH2, and MSH6 in non-tumorous gastric mucosa was

determined by immunohistochemistry. Immunostaining of four MMR proteins in the tumor tissue of the same cases (Case #13 and Case #18) are shown in Figure 2. Scale bars are 100 μm.

Supplemental Figure 4. Immunohistochemistry for MLH1 protein in intramucosal gastric carcinomas.

Representative images of immunohistochemistry in intramucosal gastric carcinomas with increased expression of MLH1. Three intramucosal gastric carcinomas (#3-2, #11-1-1, and #1-2-1) with stronger expression of MLH1 compared with non-tumorous gastric mucosa are shown. Scale bars are 500 μm or 200 μm.

Supplemental Figure 5. Overview of copy number aberrations (CNA) in intramucosal gastric carcinomas.

CNAs of intramucosal gastric carcinomas were determined using OncoScan CNV FFPE Assay Kit. Results of six representative intramucosal gastric carcinomas (synchronously developed gastric carcinomas (#1-2-1, #1-2-2) and metachronously developed gastric carcinomas (#3-1, #3-2, #10-1, and #10-2)) are shown.

Supplemental Figure 6. Focal amplifications or deletions of 30 tumor-related genes in synchronous or metachronous multiple intramucosal gastric carcinomas.

Focal amplifications or deletions of representative tumor-related genes determined in synchronous or metachronous multiple intramucosal gastric carcinomas. Thirty representative tumor-related genes were selected according to previous reports[18, 25, 26]. Red and blue boxes represent corresponding gene amplification and deletion, respectively.

Supplemental Figure 7. Comparison of CNAs among the regions of each single intramucosal gastric carcinoma.

Intra-tumor heterogeneity of CNAs detected in four intramucosal gastric carcinomas. Focal amplifications and deletions in each tumor region are shown as blue bars and red bars, respectively.

Supplemental Figure 1.

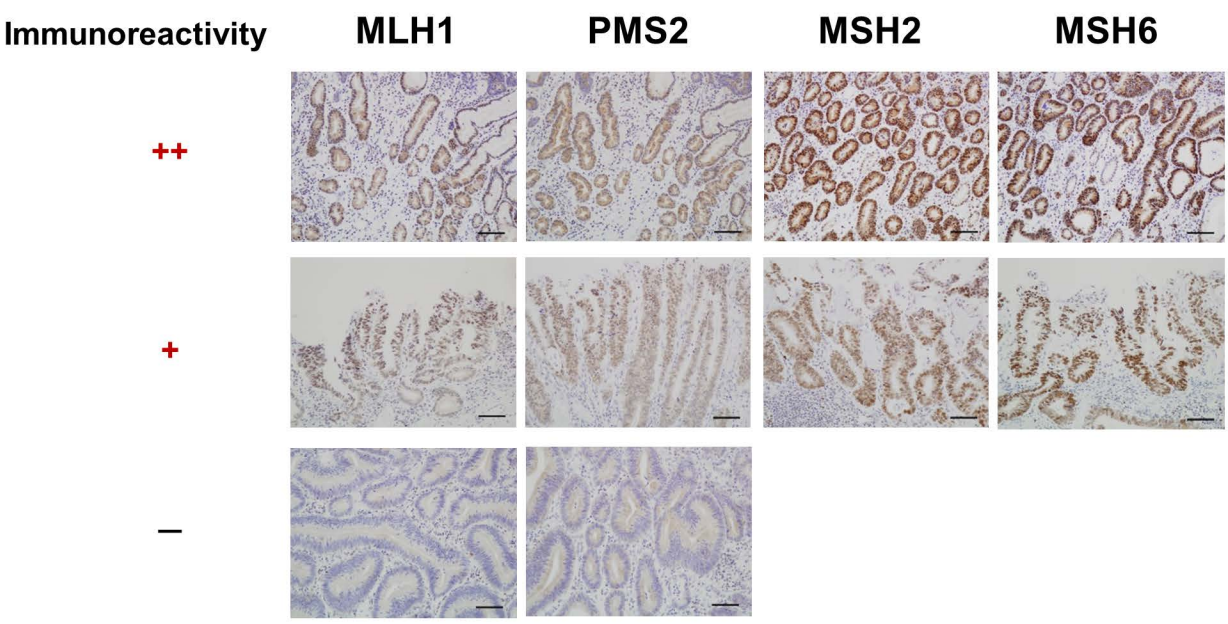

Supplemental Figure 2.

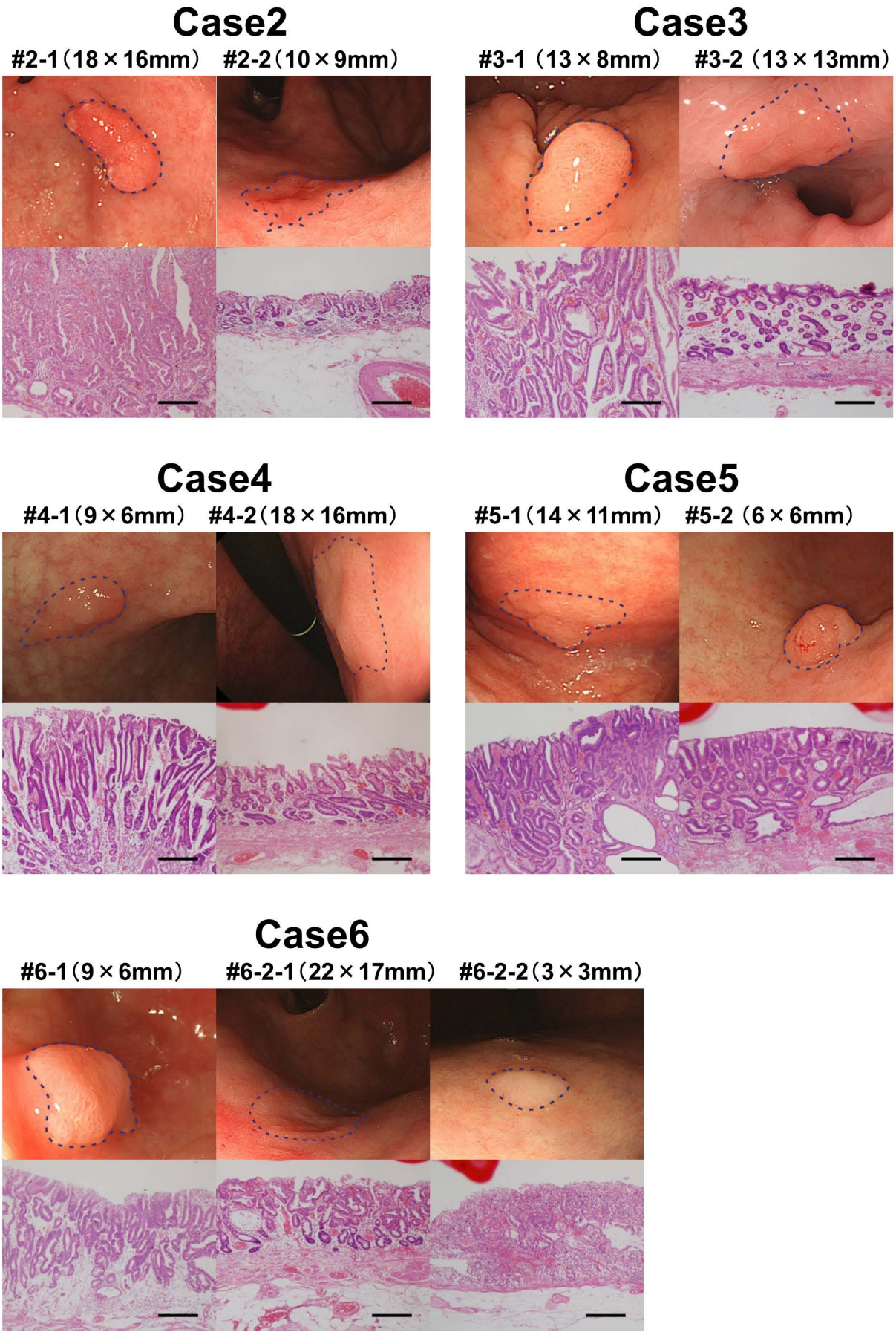

Supplemental Figure 2.

Case7

#7-1（11×8mm）　#7-2（8×7mm）

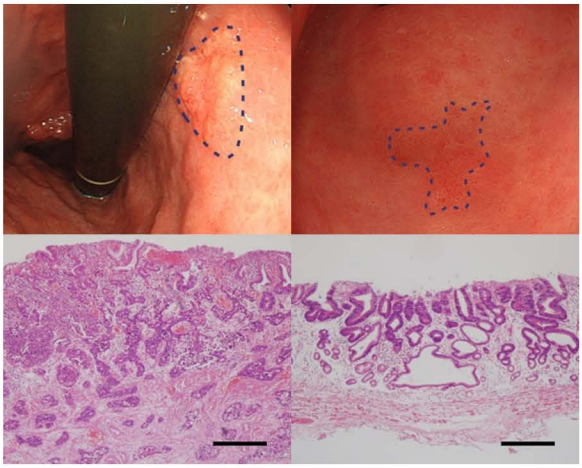

Case8

#8-1-1（16×15mm）#8-1-2（7×4mm）#8-2（8×6mm）

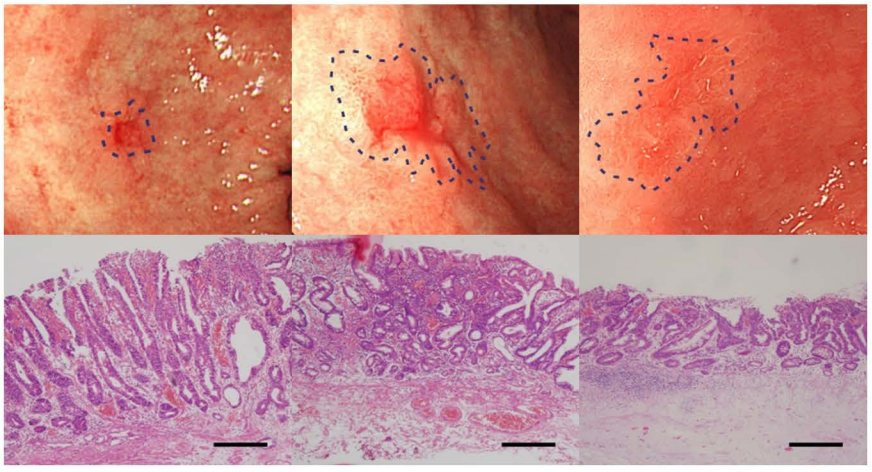

Case10

#10-1（19×15mm）#10-2（28×26mm）

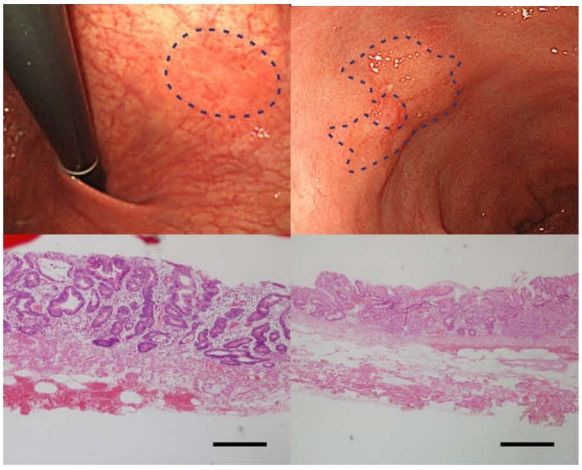

Case11

#11-1（15×11mm）　#11-2（11×7mm）

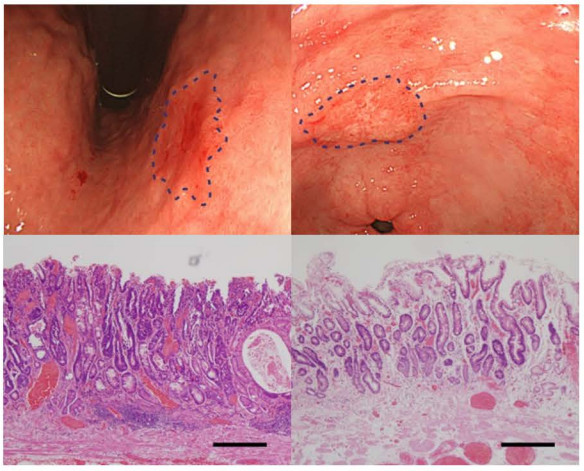

Supplemental Figure 2.

Case13

#13-1（26×12mm） #13-2（8×5mm）

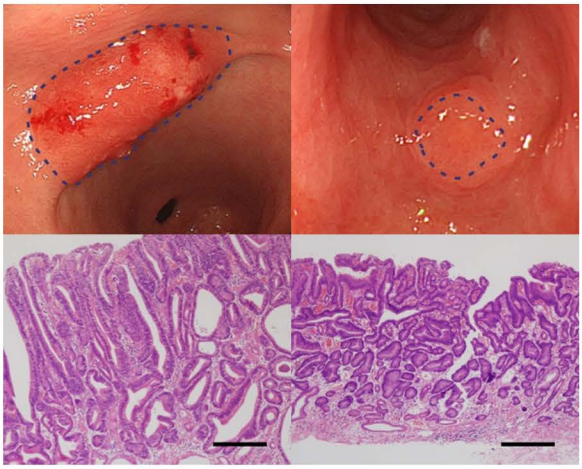

Case14

#14-1-1（20×8mm） #14-1-2（15×10mm） #14-2（7×7mm）

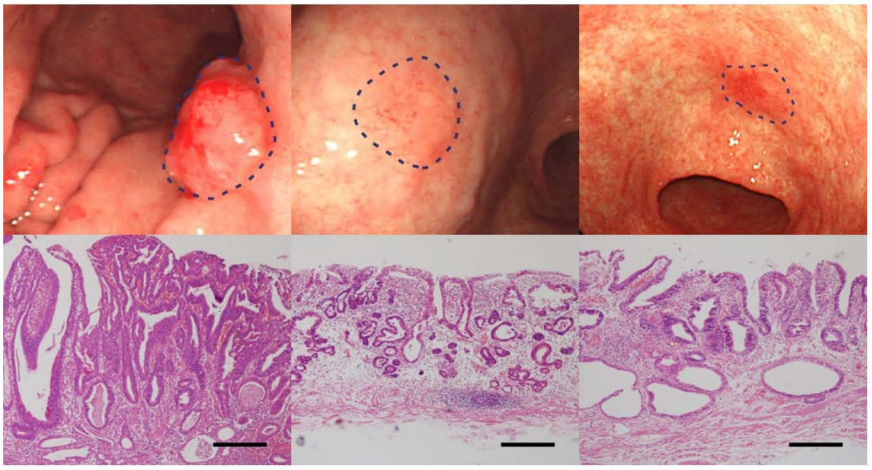

Case15

#15-1（10×8mm） #15-2（5×4mm）

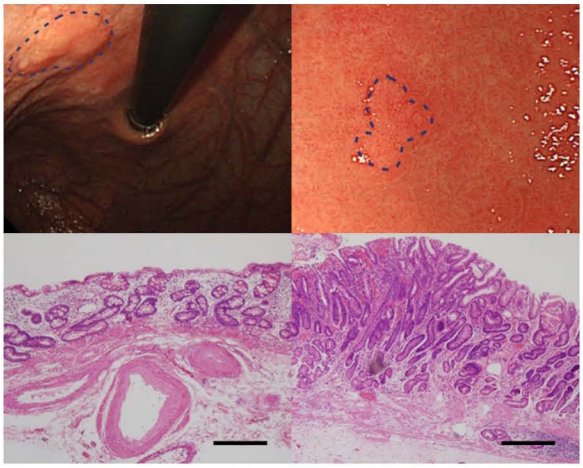

Case16

#16-2-1（6×6mm） #16-2-2（9×7mm）

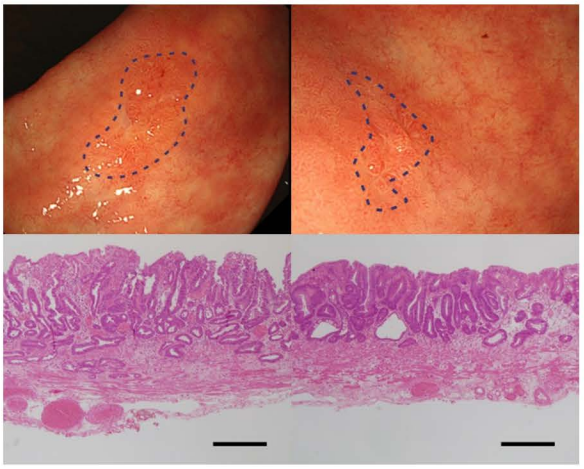

Supplemental Figure 2.

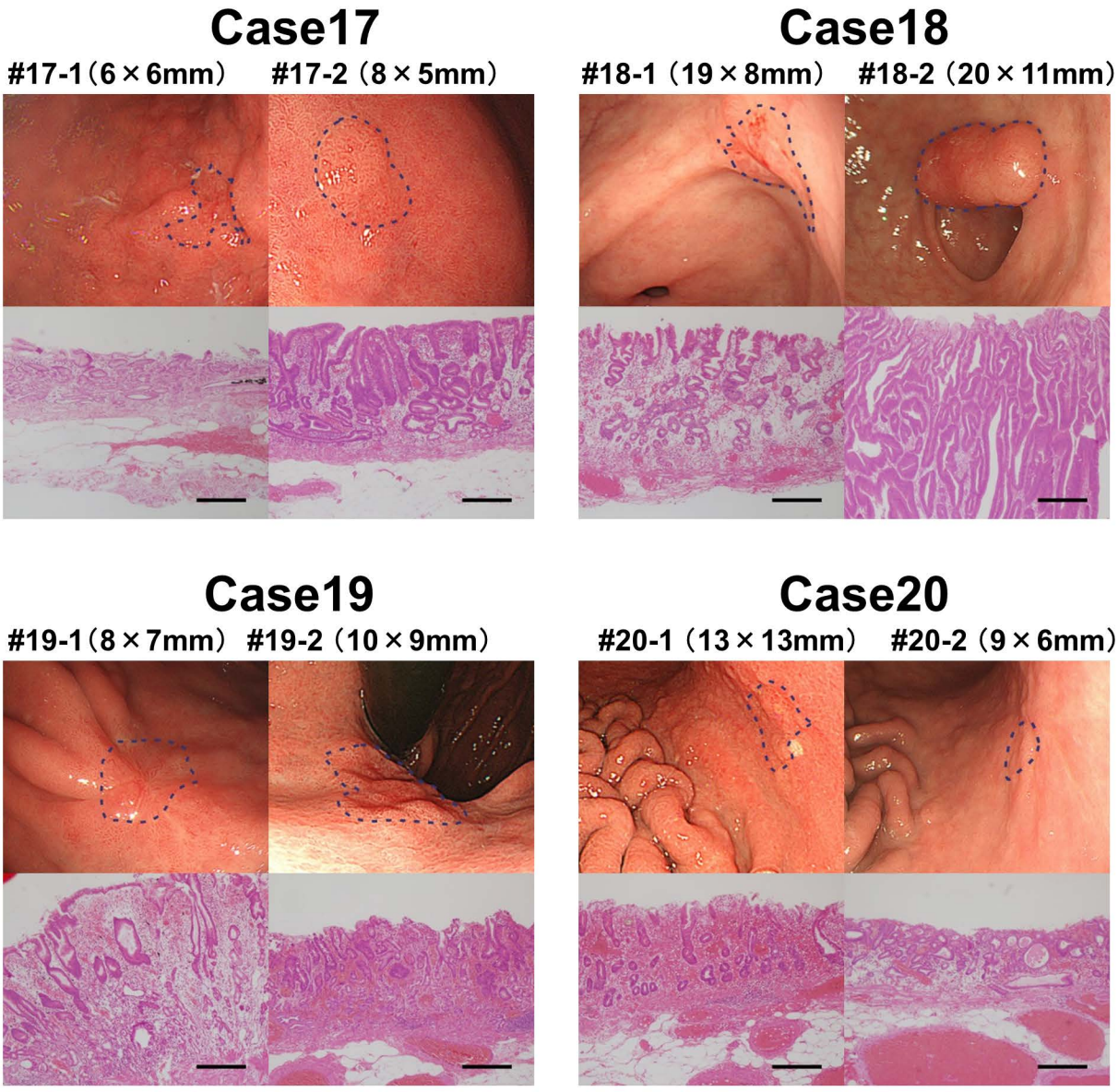

Supplemental Figure 3.

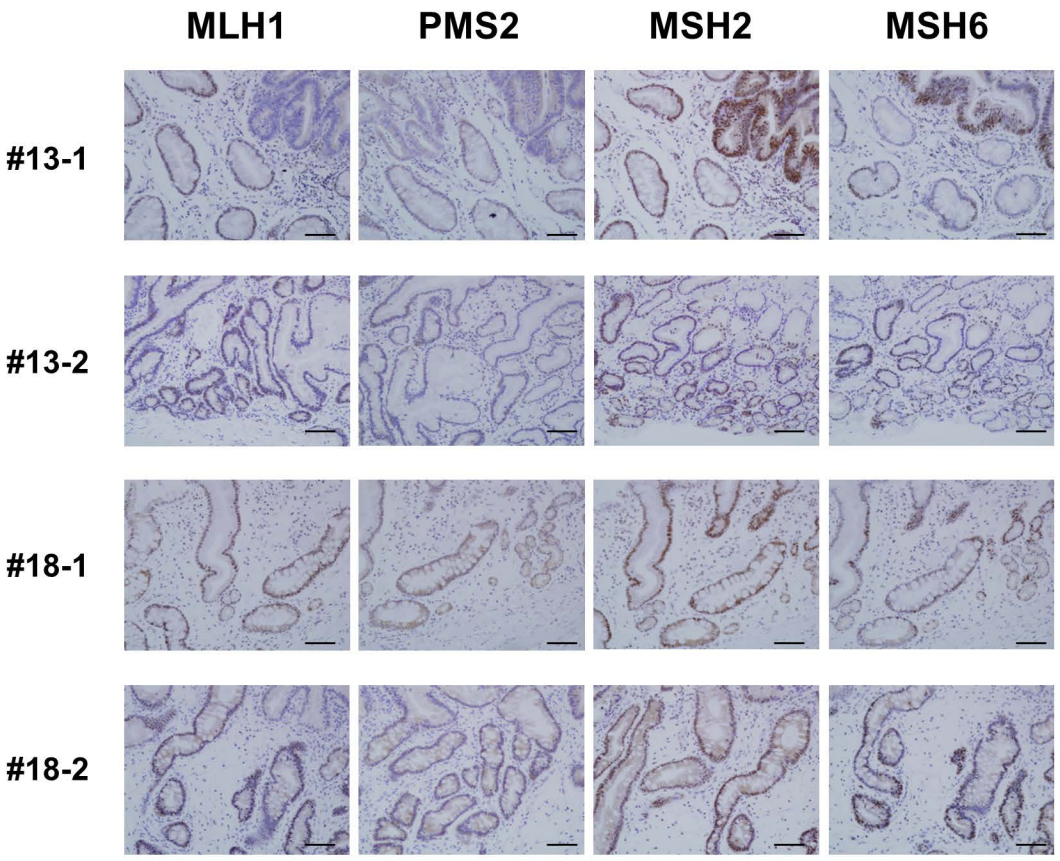

Supplemental Figure 4.

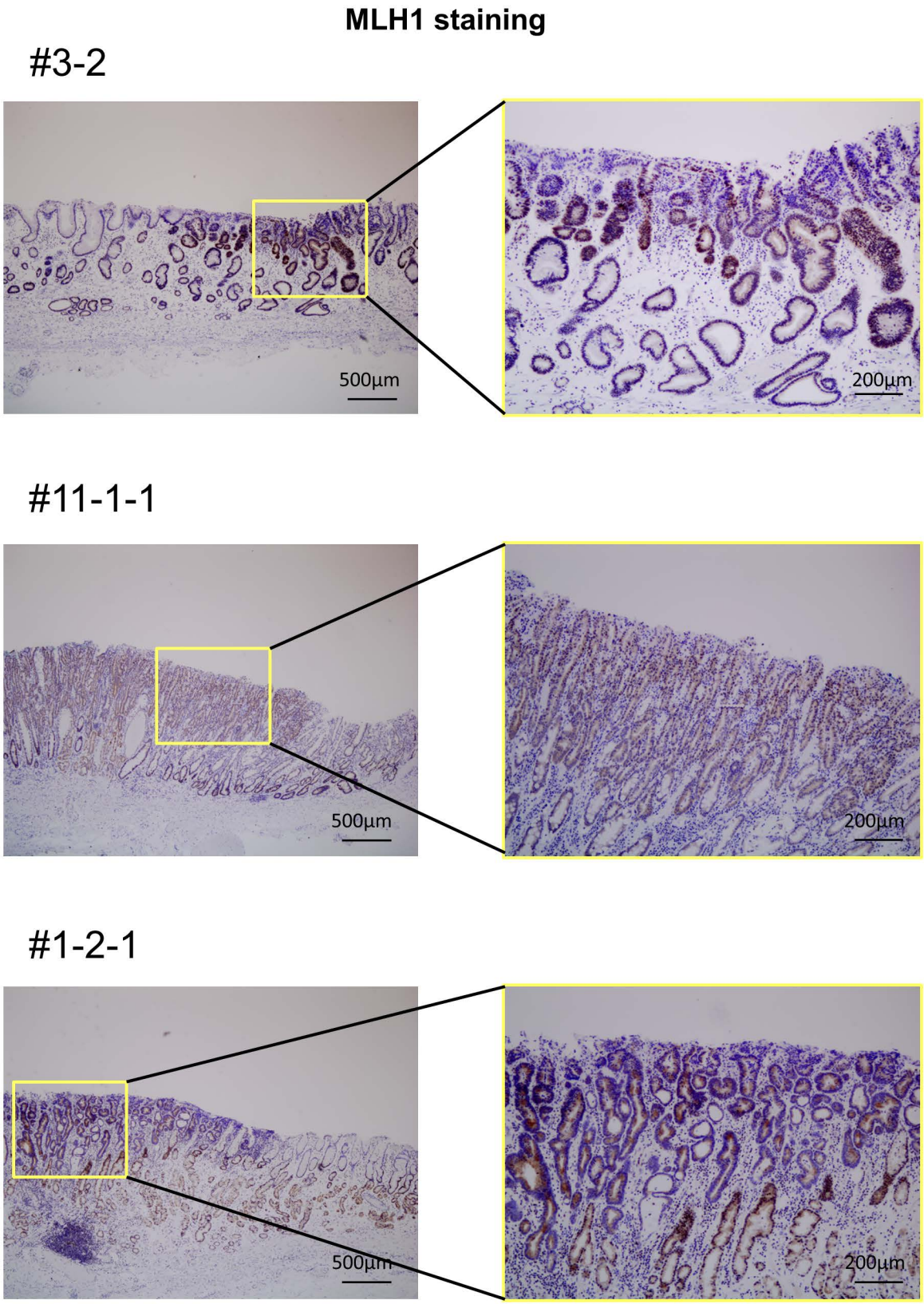

Supplemental Figure 5.

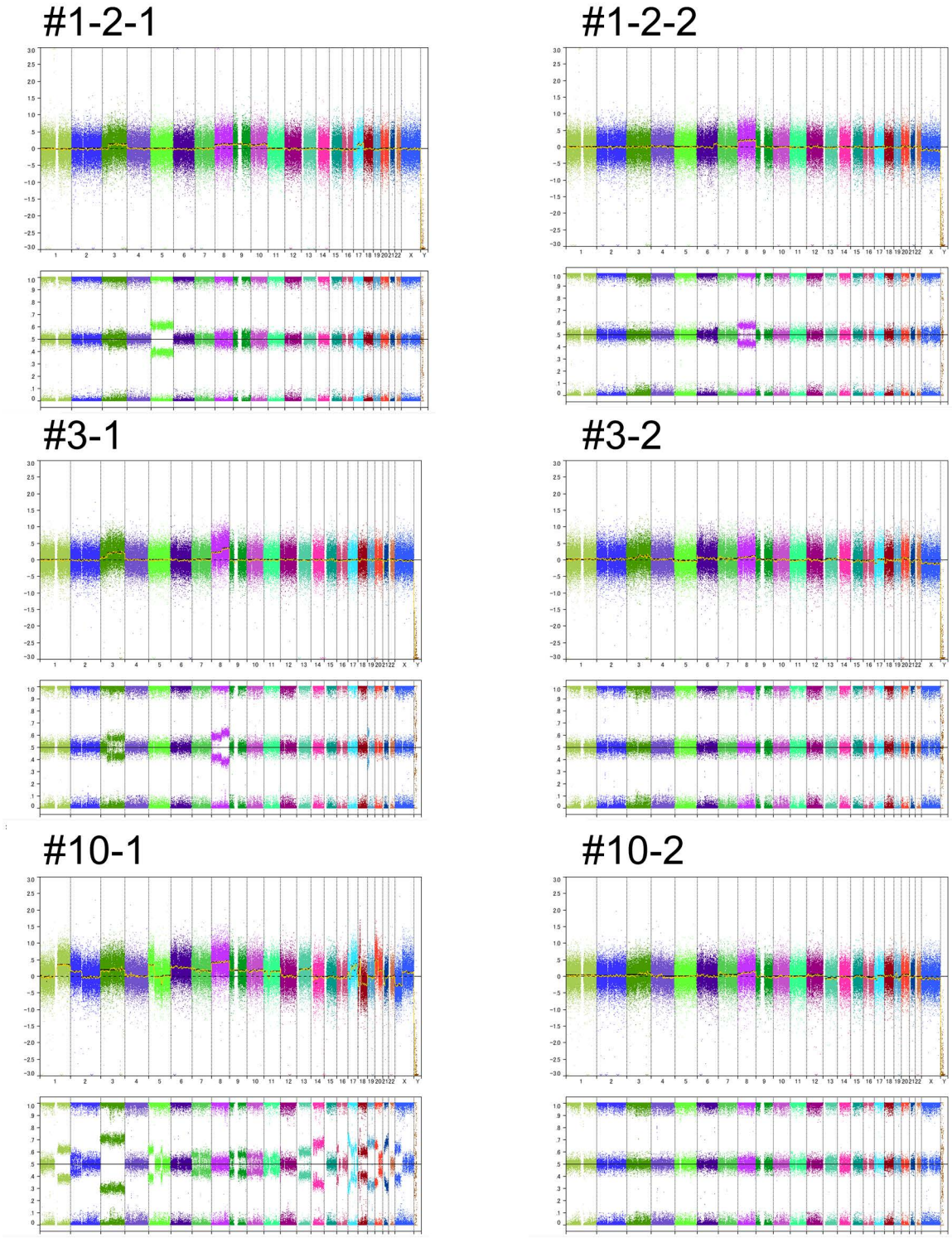

Supplemental Figure 6.

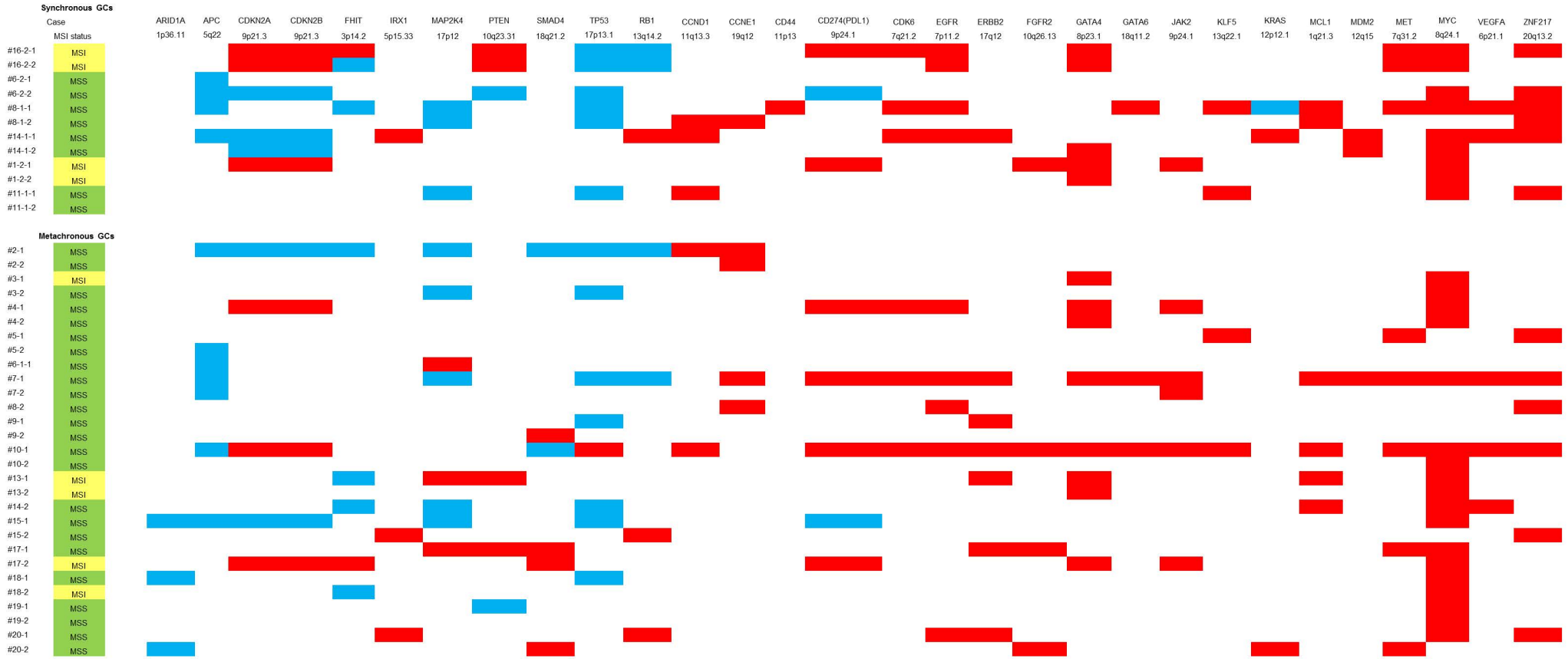

Supplemental Figure 7.

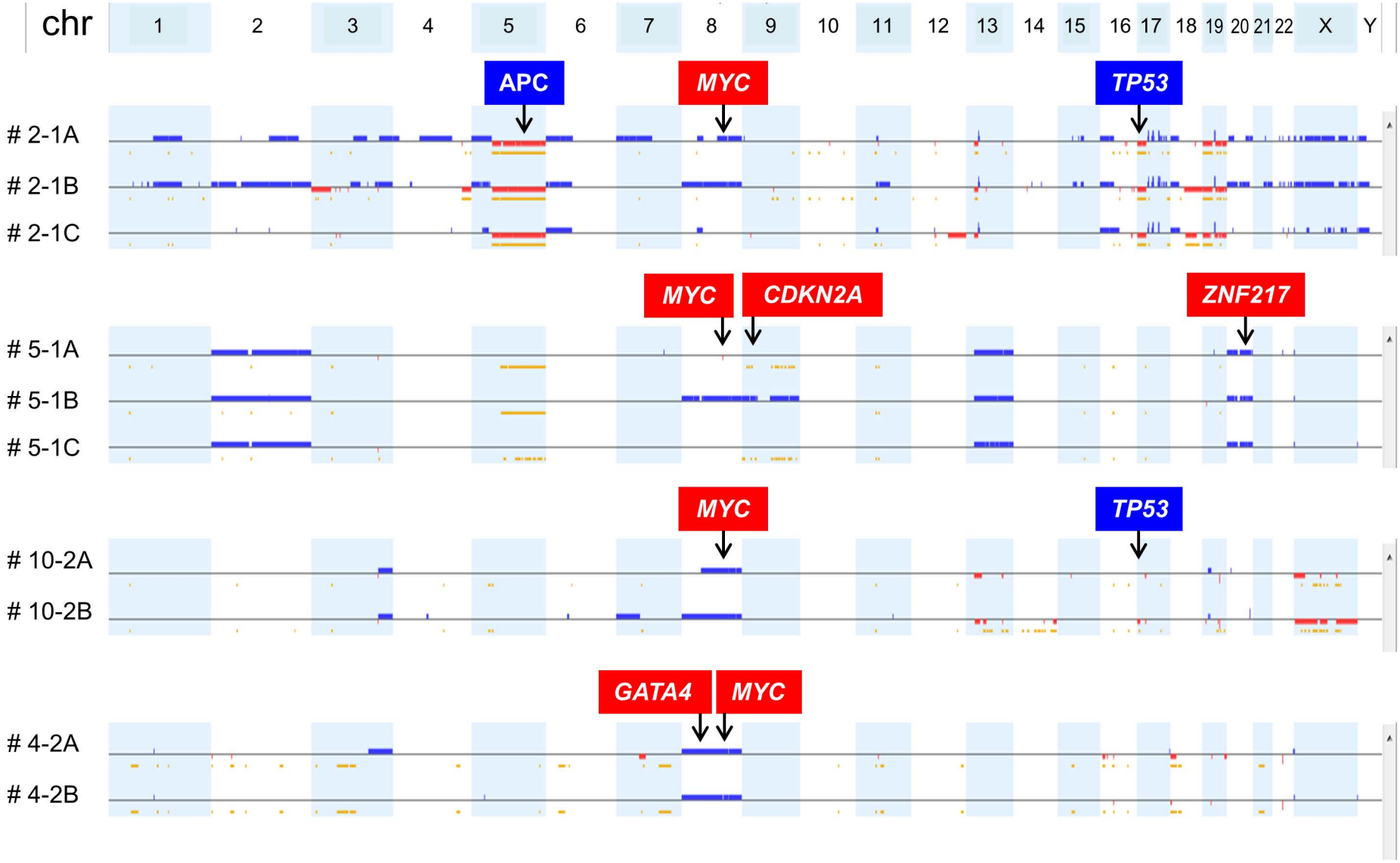

Supplemental Table 1.

Clinicopathological information of patients with synchronous multiple intramucosal gastric carcinomas

Case #	Sex	Age	Tumor	Location*	Size (mm)	Macroscopic type †	Histology ‡	MSS/MSI status §
#1	F	85	#1-2-1	M	12x12	E	tub1	MSI
			#1-2-2	L	6x3	E	tub1	MSI
#6	M	71	#6-2-1	U	22x17	D	tub2	MSS
			#6-2-2	M	3x3	E	tub2	MSS
#8	M	70	#8-1-1	L	16x15	D	tub1	MSS
			#8-1-2	L	7x4	D	tub1	MSS
#11	M	66	#11-1-1	U	15x11	D	tub1	MSS
			#11-1-2	L	11x7	D	tub1	MSS
#14	M	82	#14-1-1	M	20x18	E	tub1	MSS
			#14-1-2	L	15x10	E	tub1	MSS
#16	M	70	#16-2-1	M	6x6	E	tub1	MSI
			#16-2-2	L	9x7	D	tub1	MSI

* Location : U, upper; M, middle; L, lower

† Macroscopic type : P, protruding; E, elevated; F, flat; D, depressed

‡ Histology : tub1, well differentiated tubular adenocarcinoma; tub2, moderately differentiated tubular adenocarcinoma

§ MSS/MSI status : MSS, microsatellite stable; MSI, microsatellite instability

Supplemental Table 2.

Clinicopathological information of patients with metachronous multiple gastric carcinomas

Case #	Sex	Age	Time after PGC treatment (month)	Tumor	Location	Size (mm)	Macroscopic type	Histology	MSS/MSI status
#2	M	61		#2-1	L	18x16	P	tub1	MSS
		63	25	#2-2	U	10x9	D	tub1	MSS
#3	F	79		#3-1	L	13x8	P	tub1	MSI
		83	39	#3-2	L	13	D	tub1	MSS
#4	M	76		#4-1	L	9x6	E	tub1	MSS
		79	25	#4-2	M	18x16	D	tub1	MSS
#5	M	77		#5-1	U	14x11	E	tub1	MSS
		82	58	#5-2	L	6x6	P	tub1	MSS
#7	F	80		#7-1	M	11	D	tub1	MSS
		82	14	#7-2	L	8x7	D	tub1	MSS
#9	M	61		#9-1	M	10x10	D	tub1	MSS
		65	45	#9-2	L	11x6	D	tub1	MSS
#10	F	74		#10-1	U	NA	E	tub1	MSS
		78	49	#10-2	L	28x26	D	tub2	MSS
#13	F	86		#13-1	L	26x12	E	tub1	MSI
		90	38	#13-2	L	8x5	D	tub1	MSI
#15	M	63		#15-1	U	NA	E	tub1	MSS
		69	73	#15-2	L	5x4	D	tub1	MSS
#17	M	70		#17-1	U	6x6	D	tub1	MSS
		71	15	#17-2	M	8x5	E	tub1	MSI
#18	M	66		#18-1	L	8	D	tub2	MSS
		71	52	#18-2	L	18	E	tub1	MSI
#19	M	50		#19-1	U	8	F	tub1	MSS
		55	49	#19-2	M	10x9	D	tub1	MSS
#20	M	79		#20-1	M	13x13	D	tub1	MSS
		80	16	#20-2	M	9	E	tub1	MSS
#6*	M	70	-14 †	#6-1	L	9x6	E	tub1	MSS
#8*	M	78	100	#8-2	L	8x6	D	tub2	MSS
#14*	M	83	18	#14-2	L	7	D	tub1	MSS

*developed 3 tumors (2 tumors, synchronous; 1 tumor, metachronous)

† after 14 months from the first treatment, 2 synchronous tumors arose

PGC, primary gastric cancer